2018

Multi-robot Mission Planning with Energy Replenishment

Bingxi Li
Michigan Technological University, bingxil@mtu.edu

MULTI-ROBOT MISSION PLANNING WITH ENERGY REPLENISHMENT

By

Bingxi Li

A DISSERTATION

Submitted in partial fulfillment of the requirements for the degree of

DOCTOR OF PHILOSOPHY

In Mechanical Engineering–Engineering Mechanics

MICHIGAN TECHNOLOGICAL UNIVERSITY

2018

This dissertation has been approved in partial fulfillment of the requirements for the Degree of DOCTOR OF PHILOSOPHY in Mechanical Engineering–Engineering Mechanics.

Department of Mechanical Engineering–Engineering Mechanics

Dissertation Advisor:	*Dr. Nina Mahmoudian*
Committee Member:	*Dr. Mo Rastgaar*
Committee Member:	*Dr. Ossama Abdelkhalik*
Committee Member:	*Dr. Min Song*
Department Chair:	*Dr. William W. Predebon*

Dedication

To my parents and my wife

who always trust me, and give me love and courage.

Contents

List of Figures

List of Tables

Preface

This dissertation introduces a mission planning architecture for multi-robot systems to address long-term operation problems with energy replenishment. All work in this dissertation is done under the supervision of my advisor Dr. Nina Mahmoudian.

In general, this dissertation provides two types of multi-robot energy replenishment: static and mobile charging stations. Mission planning methods for both types of energy replenishment are developed in Chapter 2 and Chapter 4. Implementations to real-world applications validate capabilities of the proposed methods in Chapter 3 and Chapter 5.

This material is based upon work supported by National Science Foundation under grant number 1453886, and Office of Naval Research under grant number N00014-15-1-2599. The current models of Lake Michigan are kindly provided by Professor Pengfei Xue in the Department of Civil & Environmental Engineering at Michigan Technological University.

Acknowledgments

First of all, I would like to thank my advisor Dr. Nina Mahmoudian for her support and inspiring instructions through my PhD study. I would like to thank other committee members Dr. Mo Rastgaar, Dr. Ossama Abdelkhalik, and Dr. Min Song for their valuable comments and suggestions.

I would like to thank my friends at Michigan Tech and colleagues in NASLab for all the discussion, brainstorming, and fun we have in Upper Peninsula. I would like to thank my colleague Barzin Moridian, especially for his helpful criticism and insights to this work since the very beginning.

Last but not least, I would like to thank my wife Xincheng Meng for her spiritual support through my research. By the time she showed up in my life, I realized there was no problem I couldn't solve when we stand together.

Abstract

Success of numerous long-term robotic explorations in air, on the ground, and under water is dependent on the ability of the robots to operate for an extended period of time. The continuous operation of robots hinges on smart energy consumption and replenishment of the robots. This dissertation addresses the multi-robot system continuous operation problem by developing two mission planning architectures regarding two types of energy replenishment, which can be adapted to different mission scenarios based on mission requirements and available resources.

The first type of energy replenishment utilizes static charging stations to provide a recharging opportunity to primary working robots, who can periodically revisit static charging stations to be recharged through the mission. The static energy replenishment mission planning method simultaneously generates energy efficient trajectories for multiple robots and schedules energy cycling using a Genetic Algorithm (GA). The mission planning method accounts for environmental obstacles, disturbances, and can adapt to priority search distribution.

The second energy replenishment approach extends working robots operation by deploying a team of mobile charging stations to rendezvous and charge working robots. A graph transformation method is developed for mobile charging stations to solve

persistent operation problem of working robots with pre-defined trajectories. Consideration of dynamic currents effect and obstacles are integrated into the method. To optimize trajectories of both working robots and mobile charging stations, a GA based mission planning method is designed with the capability of re-planning to account for mission uncertainty.

Simulation validations are performed through solving long-term mission planning problems. A variety of real-world mission scenarios employing teams of underwater, aerial, and ground robots are simulated with multiple mission objectives under various environmental and robot constraints. The effectiveness of both developed mission planning methods in area coverage, handling energy limitations, and mission constraints are discussed and analyzed by numerical studies.

Chapter 1

Introduction

Robots have been adopted to perform dangerous and once impossible tasks in remote areas due to their capability and flexibility. The capability of robots lies in performing a variety of tasks consistently and precisely. For example, the efforts in oceanographic surveying and meteorology as well as Naval mine sweeping have been aided by teams of independent robotic workers. Multiple robots have been deployed to further improve the overall mission efficiency. However, the battery capacity and recharging needs have considerably hindered the persistent operation of robotic systems. This limitation impacts the ability to autonomously deploy robotic platforms for long-term, multi-robot missions such as immediate high-risk disaster recovery and search that requires vast area coverage.

To address the energy limitation of robotic systems, methods of introducing charging agents have been studied to increase robotic network performance. Charging agents are a team of autonomous robots or platforms capable of automating the recharging process. Carrying charging devices such as charging pads or extra energy resources such as extra batteries, charging agents can provide energy-cycling opportunities without human intervention. Based on missions requirements and objectives, the charging agent can be static or mobile.

Static charging stations can autonomously dock, recharge, and detach robots. This type of autonomous energy replenishment is appropriate for missions that have finite mission areas with periodic operations, such as surveillance and monitoring missions. Recharging stations and docking mechanisms are available for aerial and marine applications [2, 3, 4, 5, 6]. Mobile chargers are capable of autonomously repositioning within the environment and can connect to the working vehicle, fully recharge it, safely disconnect, and rendezvous with the next vehicle that needs recharging [7, 8]. This type of energy replenishment greatly improves the operational area and energy availability to working robots. As these recharging technologies advance, mission planning methods that can consider mission specifications and environmental constraints have not been studied as extensively.

This dissertation addresses the long-term multi-robot area coverage problem with both static and mobile charging stations approaches. The proposed mission planners

find multi-robot trajectories and charging station placement or deployment. Considerations of dynamic environments with constraints such as obstacles, predictable and unforeseen disturbances also integrated to the approaches to handle different mission requirements. This work also enables a trade-off study to assist mission planners in evaluating impact of parameters (number/type of working robots and charging stations) on overall mission completion time and energy cost.

1.1 Continuous Operation Utilizing Static Energy Replenishment

The traditional solution to long-term robotic missions is to manually retrieve, recharge, and redeploy vehicles. Charging station technology has been implemented to aid this process in both marine and aerial robots by enabling autonomous docking, recharging, and resuming of missions [2, 3, 4, 5, 6]. With the advancement of the technology, mission planning considering battery management and recharging and environmental constraints enables smart energy consumption and the replenishment of the robots and long-term robotic operations.

As described in [9], the battery capacity has been severely limited the aerial robots for critical missions such as search and rescue and reconnaissance missions. Therefore, many methods have been developed recently to extend the continuous operation of

robots to handle this significant constraint [9, 10, 11, 12, 13]. Getting closer to applying mission plans on real robots requires taking more realistic constraints all together compared to what is commonly addressed in the literature. Additional attention has been paid to environmental constraints as solving the long-term coverage problem without recharging possibility [14, 15]. Mainly lacking in the current work is an approach that optimizes the mission plan for both working robots and charging stations as a whole and takes into account the effect of environmental constraints on recharge time and location. Such an approach will create a multi-robot network that maintains continuous operation without the need for human intervention, and succeeds in reliably completing missions despite environmental challenges.

The contribution of this approach is the design of an energy-efficient mission planning for long-term multi-robot area coverage missions that simultaneously optimizes 1) trajectory of robots, 2) location of charging stations, and 3) recharging schedule of robots. The designed mission planning method considers robot specifications including velocity and battery capacity and characteristics of the environment including obstacles, wind/current, and regions with different coverage urgency. The novelty of this work is to merge energy replenishment problem with multi-objective coverage problem to generate efficient energy-aware mission plans.

1.2 Continuous Operation Utilizing Mobile Energy Replenishment

Although static charging systems improve the availability of energy to robots, there are still drawbacks associated with such a system. Robots need to travel back and forth to charging stations, which causes loss of energy and limits the operational area. These drawbacks are more significant for marine applications where robots are performing in inhospitable environment. Disturbances caused by environment or mission uncertainty may result in a delay or failure of robot operations, which significantly limit the efficiency of long-term missions.

The possibility of employing mobile charging stations has been studied recently. Docking between a free floating dock and a REMUS 600 has been tested [7]. It shows the possibility that a floating dock being towed by another vehicle can be adapted to an underwater mobile docking platform. Pyle et al. explored the potential of using a large AUV (Proteus) as a mobile docking/recharging station [8]. Proteus travels with working AUVs and is capable of charging two of them simultaneously. Their work combines an area coverage and an energy-depended control methodology to drive each AUV toward Proteus before the energy level becomes critical. Another effort on developing a system that facilitate autonomous docking and recharging is

the design of charging stations [16, 17]. This collapsible underwater docking system is light-weight and has a potential to be installed on Unmanned Surface Vehicles (USVs) (Figure 1.2) or AUVs to convert these vehicles to mobile power delivery systems. Figure 1.1 illustrates an area coverage scenario where two USVs are serving as mobile charging stations. There is a need for a scalable mission planning method that plans overall robotic network and recharging system considering environmental and operational constraints such as currents, obstacles, and limited communication. To improve the overall mission performance, this planner should be computationally efficient and reliable to be used online for replanning in operation.

The contribution of this work is a mission planning architecture that responds to energy consumption needs of the operating robots by deploying a team of mobile chargers in a realistic environment. Given pre-defined working robot trajectories, the mission planning method generates mobile charger trajectories using a graph transformation method considering environmental constraints such as dynamic currents and obstacles. A Genetic Algorithm (GA) based method is designed to optimize trajectories of both working robots and mobile chargers simultaneously for long-term coverage problems in uncertain conditions.

The remaining of this dissertation is organized as follow: the mission planning problem with static charging stations is formulated and detail of the approach is provided in Chapter 2. Several applications in different domains with different environmental

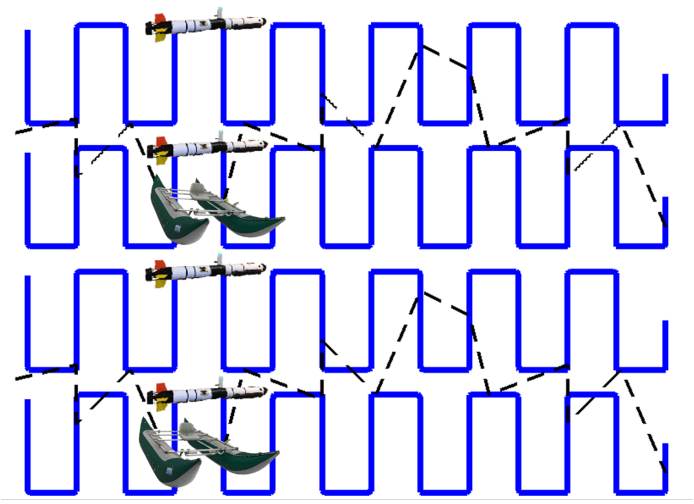

Figure 1.1: Illustration of an area coverage mission where four AUVs are following lawnmower trajectories in blue and two USVs are used as mobile charging stations following dashed lines trajectories and meeting rendezvous locations.

Figure 1.2: The AUV and USV used in a field experiment to verify the proposed method in this dissertation.

constraints using static charging stations are tested and presented in Chapter 3. The problem of mission planning using mobile charging stations is presented in Chapter 4 with the proposed approaches. Simulations are demonstrated in different scenarios with their performance discussion in Chapter 5. Chapter 6 concludes the dissertation and summarizes the future directions.

Chapter 2

Multi-Robot Mission Planning with Static Energy Replenishment

Robotic missions are usually limited in the number of robots deployed simultaneously due to difficulties in managing multiple robots and responding to the challenges. This chapter focuses on multi-robot mission planning using static charging stations for long-term operation considering multiple realistic constraints. The problem is formulated into a multi-robot area coverage problem with environmental constraints and solved by a greedy algorithm and a Genetic Algorithm (GA).

2.1 Related Work

This section reviews related literature, including the complete coverage problem, the multi-robot recharging problem, and mission planning considering environmental constraints.

A comprehensive survey reviewing the most successful methods to generate robot trajectories for Coverage Path Planning (CPP) problem is presented in [18]. Grid-based methods use uniform grid cells to represent the mission area, first brought up in [19] as an approximate cellular decomposition. The grid-based method has been used for CPP using different algorithms such as the Wavefront Algorithm [20], Spanning Trees [21], and the Neural Network-based approach [22]. While we use the grid-based map approach, instead of finding the trajectory for a mobile robot, we consider both multi-robot trajectories as well as their recharging schedules and locations. The mission planning problem for persistent coverage, exploration, and surveillance missions with multiple robots has been studied [9, 10, 11, 12, 23, 24, 25, 26, 27, 28, 29]. Using heuristic methods to respond to mission specifications is common in multi-robot area coverage mission planning [11, 12, 15, 24, 25, 29]. Unlike persistent coverage problems that attempt to maintain a desired coverage level for a mission area over infinite time, the coverage model in this work does not require revisiting mission points.

Planning long-term robotic missions requires replenishment of robots' batteries. The concept of mission planning considering recharging constraints has been studied using mobile chargers [11, 29, 30, 31, 32]. Charging multiple working robots using a tanker that meets working robots for a recharge during their mission has been studied [30]. How to efficiently reach working robots has also been addressed [31, 32]. Using a team of service robots that carry energy to recharge working robots has been studied as well [11, 29]. These methods assume pre-defined trajectories of working robots and do not consider the constraints imposed by the environment.

Prior work on the coverage problem with recharging limitation and scheduling is either valid for only one mobile robot [33], or responds to the energy limitation by offering one fixed charger dedicated to each working robot without sharing [12]. An algorithm to solve the multi-robot persistent coverage problem is proposed in [12], optimizing the path for a fleet of robots visiting all the targets while maintaining an adequate fuel capacity by refueling at depots placed at fixed locations [12]. Optimizing the worker path and placement of mobile recharging stations jointly is studied in [33] using a two-step optimization with greedy algorithms for a fuel constrained aerial robot and a refueling ground vehicle. Their work can only consider a single working robot with a single charging robot, although the greedy algorithms are employed to reduce the computational time. Similarly, the problem of handling different robots sharing different depots is not addressed in [12]. Our work addresses the problem of multiple robot trajectories planning with shared charging stations.

The mission planning problem using static charging stations is also close to the Multi-Depot Vehicle Routing Problem (MDVRP) in terms of the limited capacity mission planning problem. In the MDVRP, multiple vehicles are deployed from multiple depots to deliver the product to the customers. The vehicles have limited capacity. They need to return to the same depot where they start to refill. Each customer can have a different demand. MDVRP is a NP-hard problem, and finding the optimal solution is extremely time-consuming [34]. Usually heuristic methods such as Genetic Algorithms are used to find a solution by solving three decision problems (grouping, routing, and scheduling) [34, 35]. However, the developed methods for MDVRP cannot be used for our problem because the locations of depots in MDVRP are pre-defined. In addition, no method can handle multiple vehicles sharing the depots in MDVRP.

Some efforts have focused on developing mission planning methods for multi-robot persistent surveillance missions utilizing shared charging stations [9, 10]. The method results in an online and offline control policy for motion planning of a team of aerial robots using charging stations [10]. The experiment with three charging stations in a target area shows the effectiveness in increasing mission time of the proposed system with a limited number of mission points, however the robot trajectory optimization is not discussed [9]. Although, many studies consider the problem of multi-robot trajectory optimization and placement of charging stations from different aspects, none takes into account all the constraints together.

Environmental challenges such as obstacles are considered in some mission planning works [20, 21, 22, 26, 36]. In grid-based coverage problems, the obstacles are usually bounded in the mission area so that the proposed approaches are capable of avoiding the obstacles [15, 20, 21, 22]. In our problem, obstacle avoidance is not achieved by the formation of the proposed method. Instead, we use a penalty function to eliminate infeasible paths. In most mission planning literature, less attention has been paid to environmental constraints such as wind and currents which are crucial for real-world missions especially in the air and sea. For underwater vehicles path planning in long-term missions, the energy cost is usually estimated by the vehicle's velocity vector and current vector in two-dimensional maps [37, 38]. In [37], the time-based heuristic cost is estimated by choosing the direction of gliders velocity and finding the resultant net velocity between the predicted current vector and the glider vector on a grid-based map. To handle the time-varying flow, a graph-based approach is presented in [38]. We follow the same method in this work to find the energy cost under the known current effect.

2.2 Problem Statement

The aim is to find the positions of charging stations as well as trajectories of working robots while they visit all the mission points with the minimum energy spent and satisfy the environmental constraints.

The number of working robots is represented with W and the charging stations with C. All working robots have the same energy capacity G and the same maximum speed. The energy costs of the working robot trajectories are calculated by the distance and the speed of the robots under the current ($\vec{Cr}$) effect. The charging stations are placed on vertices in the mission area. Working robots need to revisit those vertices to recharge their batteries. The energy limit constraint for the working robots is that the energy costs of working robots visiting two consecutive charging stations must not exceed G. It is assumed that the charging stations have unlimited energy, and the energy cost of working robots has a linear relation with their operation time.

Given the prior information about the mission area $M \subset \mathbb{R}^2$, a grid-based approach is used to represent the mission area and the obstacle area using uniform cells. The mission area is given as a directed graph $\mathbb{G}(V, A, p, B, \vec{Cr})$, where V is the set of vertices, A is the set of edges, $p : V \to \mathbb{R}$ is a distribution function that assigns a priority value to each vertex in V, B is the set of obstacle vertices, and $\vec{Cr}$ is the current model. The vertices are the mission points that need to be visited by working robots. Each edge $a_{i,j} \in A$ is an ordered pair of vertices (v_i, v_j) with the assigned direction from v_i to v_j. A trajectory of working robots is a sequence of edges and the energy cost of this trajectory is the summation of the cost of all the edges in the trajectory. To guarantee the full coverage of the mission area, all vertices (V) should be visited at least once by a working robot.

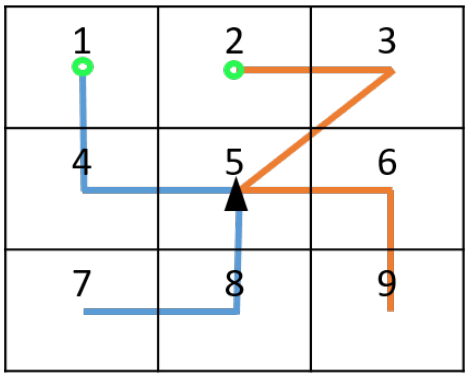

Figure 2.1: An example of two working robots covering the mission area with the support of one charging station. The robots respond to their energy limitation constraint by visiting the charging station.

To illustrate the definitions and constraints, consider a mission area with two working robots ($W = 2$) and one charging station ($C = 1$) shown in Figure 2.1. The goal is to place the static charging station and find the working robot trajectories with the minimum energy spent. The mission area is discretized in 9 uniform cells. The energy cost of working robots is defined as the distance each robot travels. The energy capacity for working robots is enough for traveling 3 unit distances (for example, we consider the cost of traveling from cell 5 to cell 2 as 1 unit distance, and from cell 5 to cell 1 as 1.41 unit distances). The trajectories of working robots visiting all 9 vertices while avoiding being completely discharged by visiting the charging station vertex are shown as blue and red lines in the figure. For the presented solution, the charging station is placed at cell 5 shown by the black triangle. The energy cost associated with the trajectory of the first working robot (blue line) is $(1, 1, 1, 1)$ and remaining energy level is $(2, 1, 2, 1)$. For the second working robot's trajectory (red line), the energy cost is $(1, 1.41, 1, 1)$ and remaining energy level is $(2, 0.59, 2, 1)$. The

total energy cost is $(1+1+1+1)+(1+1.41+1+1)=8.41$ unit distances.

2.3 Mission Planning Approaches with Static Energy Replenishment

A Genetic Algorithm (GA) is designed in Section 2.3.1. to optimize the trajectory planning problem and charging stations placement problem together considering environmental constraints. As a comparison, we propose a greedy algorithm to solve charging stations placement problem and the trajectory planning problem in two steps in Section 2.3.2.

2.3.1 Genetic Algorithm

GAs have been successfully implemented for trajectory optimization problems in recent years [15, 34, 35, 39, 40]. GA is an evolutionary algorithm that keeps the population of candidate solutions evolving to better solutions under selective pressure based on fitness.

As shown in the flowchart (Figure 2.2), we first consider the effect of environmental constraints such as obstacles and currents in finding working robots trajectories

and associated energy costs. Then, the encoding and decoding of working robots trajectories and charging station locations take place in the initialization process. The mission objectives and constraints are then used to find the fitness value in the evaluation and selection process. The crossover process produces the new generation. Post-processing provides the solution to the problem after the algorithm stops. The details of each process are presented in the following sections.

2.3.1.1 Environmental Constraints Consideration

Considering the environmental constraints such as current and obstacles will impact energy costs for traveling in the mission area. The mission area is discretized using uniform cells with N vertices to represent those cells

$$V = \{v_1, \ldots, v_N\}.$$

The size of the cell is decided by the requirement of the mission such as the sensor range or desired sampling resolution. The Euclidean distance between every two mission points is calculated,

$$D = \{d_{i,j} : i, j = 1, \ldots, N\},$$

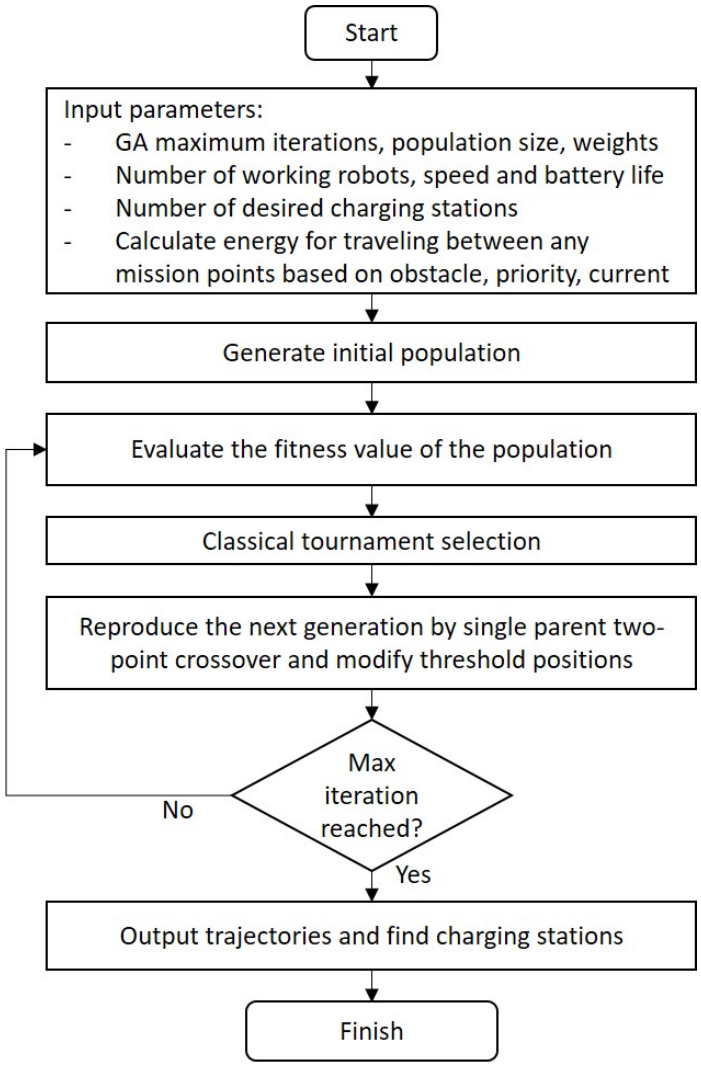

Figure 2.2: The steps of solving the mission planning problem using the genetic algorithm for finding energy efficient trajectories of working robots and positioning of the charging stations considering environmental constraints.

where $d_{i,j}$ is the Euclidean distance between mission points v_i and v_j. To calculate the energy costs of all the edges, we first find the velocities of the robots traveling under the current effect. Then the energy costs are calculated using the travel distance and the velocity.

The effect of current or wind in the mission area is represented by $\vec{Cr}$. The magnitude

($\|\vec{Cr}\|$) defines the current or wind speed. Here, we consider an evenly distributed, unidirectional, and constant $\vec{Cr}$ in the mission area. It is assumed that the robots travel at the same speed ($\|\vec{s}_{out}\|$), and change their headings to accommodate the current effect (Figure 2.3).

For each edge $a_{i,j} \in A$, given $\|\vec{s}_{out}\|$, $\vec{Cr}$, and the direction of $\vec{s}_{i,j}$, the velocity of working robots ($\|\vec{s}_{i,j}\|$) under the current effect can be calculated by

$$\vec{s}_{i,j} = \vec{s}_{out} + \vec{Cr}.$$

The set of the velocity for all edges is $\{\|\vec{s_{i,j}}\| : i, j = 1, \ldots, N\}$ where $\|\vec{s_{i,j}}\|$ is calculated by

$$\|\vec{s_{i,j}}\| = cos\alpha_1\|\vec{s}_{out}\| + cos\alpha_2\|\vec{Cr}\|.$$

α_1 is the angle between the desired travel direction and the robot's heading,

$$\alpha_1 = arcsin(sin\alpha_2\|\vec{Cr}\|/\|\vec{s}_{out}\|),$$

and α_2 is the angle between the desired travel direction $\vec{s}_{i,j}$ and the current $\vec{Cr}$.

The travel time for each edge can be calculated by $t_{i,j} = d_{i,j}/\|\vec{s_{i,j}}\|$. The set of energy costs $U = \{u_{i,j} : i, j = 1, \ldots, N\}$ is linear with the travel time $u_{i,j} = \gamma t_{i,j}$.

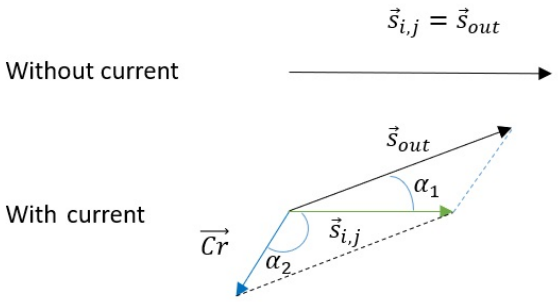

Figure 2.3: The current changes direction of the travel of the working robot. α_1 is the angle between the desired travel direction and the robot's heading, and α_2 is the angle between the desired travel direction and the current.

To account for obstacles in the mission area, the algorithm verifies if the edge $a_{i,j} = (v_i, v_j)$ crosses through the obstacle area by checking if any of the corresponding cells belong to the obstacle area (B). An edge (v_i, v_j) connects the start point (x_a, y_a) to the end point (x_b, y_b), where x_a, x_b, y_a, y_b are the x and y positions of v_i and v_j in a 2D coordinate. To find the corresponding cells for (v_i, v_j), we interpolate (x_a, y_a) and (x_b, y_b) by N_b points

$$[(x_a, y_a), (x_a + \delta x, y_a + \delta y), (x_a + 2\delta x, y_a + 2\delta y), (x_a + N_b\delta x, y_a + N_b\delta y)],$$

where $N_b = 2\sqrt{(x_a - x_b)^2 + (y_a - y_b)^2}$, $\delta x = (x_b - x_a)/N_b$, and $\delta y = (y_b - y_a)/N_b$. Then, the nearest cells to each interpolation point are the corresponding cells to this edge. If an edge crosses through B, then a large penalty will be added to the

pre-calculated edge cost.

$$u_{i,j} = \begin{cases} \infty, \text{ if } a_{i,j} \text{ crosses } B \\ u_{i,j}, \text{ otherwise.} \end{cases}$$

2.3.1.2 Initialization

In this process, a population of much larger than N chromosomes is randomly generated. A fixed-length decimal encoding is applied to the chromosomes. N mission points are labeled. Each chromosome has N genes. Each gene indicates a mission point and the order of the genes in a chromosome represents the trajectories of robots. For multiple robots, the chromosome is evenly divided to represent the trajectories of different robots (Figure 2.4).

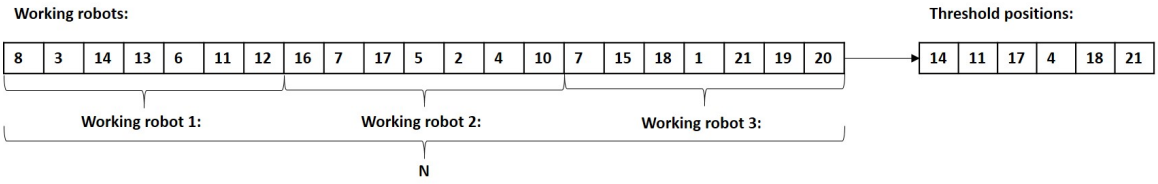

Figure 2.4: Each chromosome represents the trajectories of working robots, together with the threshold positions selected by a random selection.

Working robots operate in working and recharging phases. Before the battery life of a working robot reaches a critical level, it needs to pause the coverage mission, leave the mission path, and travel to a charging station. Threshold positions (TP)

are the locations from where the working robot will start heading to a charging station. Taking advantage of the grid-based representation of the mission area, we can calculate the maximum mission points a working robot can visit with a single battery life (N_t). A number is randomly chosen from [1 .. N_t] for each threshold position to accommodate the energy limit constraint.

Using a fixed-length decimal chromosome to represent the mission area is a widely used model to convert maps in discrete mathematical operations [39]. The advantage of this encoding method is that the full coverage constraint is automatically satisfied. The disadvantage is that the classic two parents crossover and mutation methods cannot be used since they produce unfeasible children (some mission points are not visited and some mission points are visited more than once).

2.3.1.3 Evaluation

In the evaluation process, we calculate the fitness values of the chromosomes. The weighted sum approach is used to convert the multi-objective optimization problem into a single objective optimization problem. The weighted sum approach is very computationally efficient and easy to implement [41]. Finding the Pareto-optimal solution is not of interest in this work.

The fitness function (FF) is expressed as

$$FF = w_1 E + w_2 L + w_3 H + w_4 P \tag{2.1}$$

where E represents the total energy consumption, L denotes the penalty of violating the energy limit constraint, H minimizes the distance between threshold positions, and P minimizes the time to cover any high priority search areas. w_i is the weight for each mission objective. The combination of weights usually are chosen after multiple runs.

To calculate the energy consumption and verify the energy limitation constraint, we analyze the trajectories of W working robots, and check each segment of these trajectories. We divide each trajectory into multiple segments by threshold positions. Each segment represents the trajectory a working robot travels between two consecutive visits of charging stations with one battery life. We denote trajectories of W working robots as $R = \{R_{i,j} : i = 1, \ldots, W, j \in \mathbb{N}\}$, where $R_{i,j}$ is the jth segment of the ith working robot trajectory. For example, segment 1 of the first working robot trajectory is denoted as $R_{1,1} = (a_{1,2}, a_{2,3}, \ldots, a_{k,k+1}) : a_{i,j} \in A$, associated with the set of energy cost $E_{1,1} = (u_{1,2}, u_{2,3}, \ldots, u_{k,k+1}) : u_{i,j} \in U$.

The total energy consumption of all robots is

$$E = \sum_{i=1}^{W} \sum_{j} E_{i,j}. \tag{2.2}$$

The penalty of violating energy limit constraint is expressed as

$$L = \sum_{i=1}^{W} \sum_{j} \begin{cases} 0, \ E_{i,j} \leq G \\ \\ E_{i,j} - G, \ E_{i,j} > G. \end{cases} \tag{2.3}$$

When the number of threshold positions (TP) is larger than the desired number of charging stations C, we divide TP into C groups $TP = \{TP_1, \ldots, TP_C\}$. For each group, the distance between all threshold positions is minimized so that they can be combined as a charging station

$$H = \sum_{n=1}^{C} \sum_{i,j \in TP_n} d_{i,j}, \text{ where } d_{i,j} \in D. \tag{2.4}$$

In search missions, high priority areas are usually areas of map with a higher success rate which can conclude the search mission without covering the full area. To consider the priority of coverage during mission planning, each mission point v_i is assigned with a priority value p_i based on a given probability distribution and is expected to

be visited at t_i time step

$$P = \sum_{i=1}^{N} p_i t_i. \tag{2.5}$$

The weight of these four mission objectives in the fitness function define the importance of each objective in the optimization. Minimizing energy consumption is the primary goal in contrast with the time covering the high priority area as a secondary goal, therefore w_1 is larger than w_4. w_2 and w_3 impact how much the algorithm penalizes the candidate solutions which violate energy limitation and have large distance between threshold positions. The value for w_2 and w_3 should be large enough to find the solution that does not violate the energy limitation constraint with the desired distance between threshold positions.

2.3.1.4 Selection and Crossover

Using tournament selection, one eighth of chromosomes are selected as parents for generating new chromosomes. A two-point single-parent crossover is applied to half of the parents, for which the two points are selected from anywhere on the chromosome. For the other half, the crossover is performed for two points that are selected from a segment of parent chromosome that represents the trajectory of a single robot.

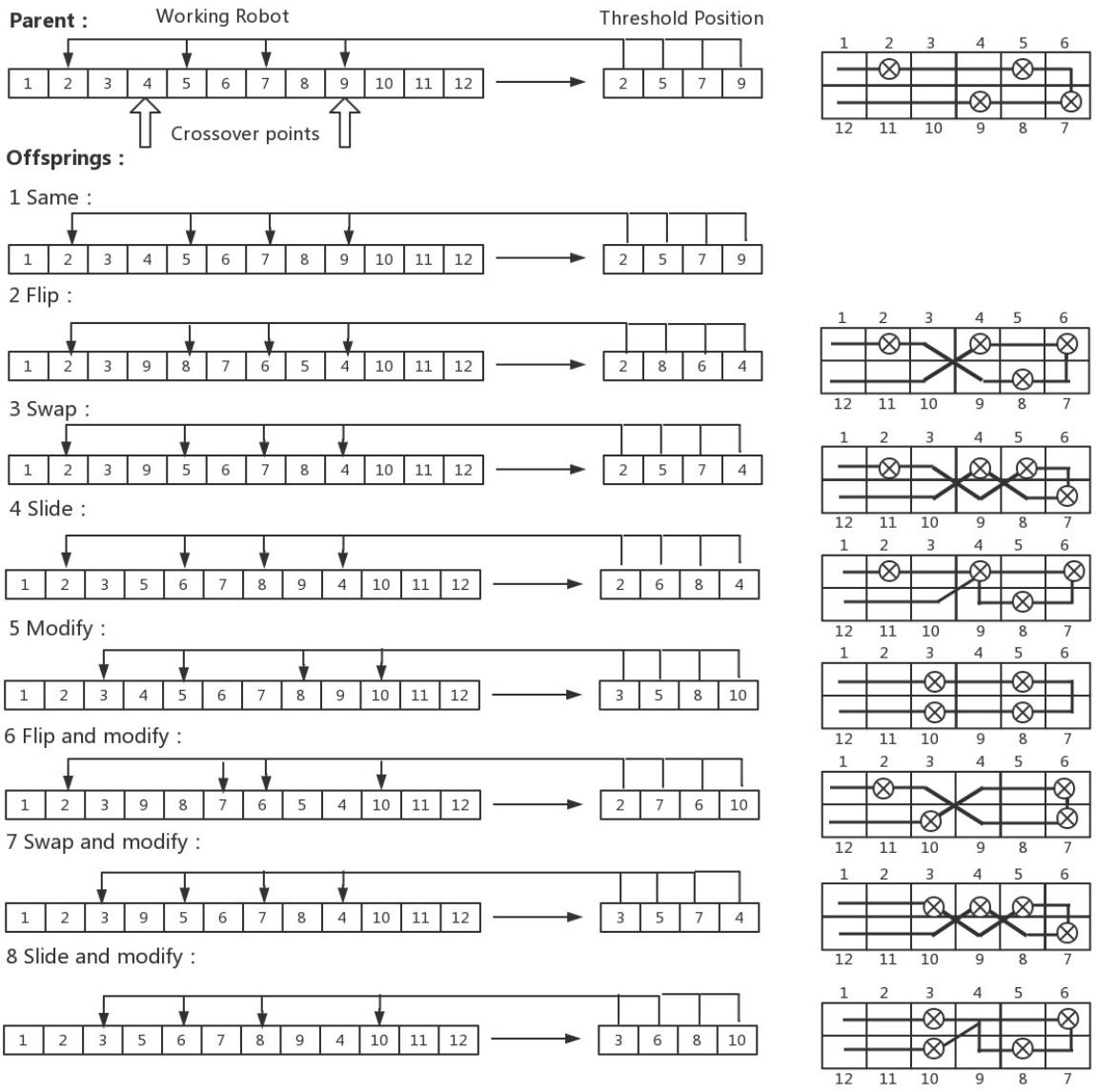

Figure 2.5: The population reproduction uses a single parent two-point crossover process [1]. The illustrations of the decoding of each offspring are shown on the right.

The crossover comprises flipping, swapping, or sliding the two selected points (Figure 2.5). The threshold positions for each offspring chromosome are either kept at the same gene positions or randomly relocated to new gene positions. Modifying the threshold position facilitates the battery life constraint (Eqn. 2.3). The locations of

the charging stations are assigned based on the threshold positions. The crossover grows the number of chromosomes eight times, keeping the size of population constant from one iteration to next.

2.3.1.5 Post-process

The iterations stop when the simulation meets the maximum number of iterations. The maximum number of iteration is determined by running the algorithm multiple times to find the convergence of the results. The chromosome representing the trajectories of working robots and threshold positions with the lowest fitness value (FF) is the output of the algorithm.

To find the best positioning for charging stations (C), the threshold positions (TP) are checked and analyzed following these steps: 1) the number of other threshold positions within the radius of a unit distance are found for each threshold position. 2) The threshold position with the largest number of neighbors is selected, and combined with its surrounding threshold positions as a charging station. Repeat the first two steps until all the threshold positions are assigned.

2.3.2 Greedy Algorithm

A two-step greedy algorithm is employed for energy-efficient mission planning using static charging stations. Given the mission area, the number of working robots and charging stations, we first use the k-means clustering [42] to find the locations of the charging stations. Then a nearest neighbor algorithm similar to [33] is used to find the trajectories of the working robots.

To place the static charging stations, given N mission points and C charging stations, the k-means clustering algorithm partitions the mission points into C clusters. The centroid of each cluster is the location of a charging station. The k-means clustering algorithm alternates between the assignment step and the update step in each iteration. In the assignment step, each mission point is assigned to the cluster whose centroid has the least squared Euclidean distance. Then, the new centroids are found in the update step. The iterations continue until the convergence of the results.

Next, a nearest neighbor algorithm is applied to find the trajectories of working robots based on the location of the charging stations. In each iteration, this algorithm finds the nearest mission points relative to the current working robot positions and the nearest charging stations to the nearest points. It also calculates the corresponding required energy for reaching the nearest point and the charging station. If the required

energy is less than the available energy of the working robot, it goes to the nearest point. Otherwise, the working robot travels to the nearest charging station directly. The algorithm continues to find working robot trajectories until all the mission points are visited or all the working robots have no point to move.

Chapter 3

Mission Planning Applications with Static Energy Replenishment

The capabilities of the developed mission planning method, especially in handling multiple environmental constraints, are examined in this chapter. Three mission scenarios with different scales and environmental constraints employing ground, aerial, and underwater robots are used to verify the proposed mission planning method.

In Section 3.1, the proposed method is implemented into a sample area coverage mission scenario similar to the MH370 airplane search mission [43]. The simulation results considering mission objectives and constraints such as the priority area, obstacles, and currents are presented. The presented method is evaluated through Monte

Carlo simulation using different number of working robots where the mission cost and success rate is compared.

In Section 3.2, the proposed method is implemented and tested in the simulation of a search and rescue mission in Yosemite National Park using Unmanned Aerial Vehicles (UAVs) and charging stations [44]. The simulation results and the Monte Carlo evaluation in MATLAB are discussed.

In Section 3.3, an oil spill detection mission planning problem with similar mission area to 1969 Santa Barbara oil spill accident is simulated with Autonomous Underwater Vehicles (AUVs) and Autonomous Surface Vehicles (ASVs) [45]. The mission scenarios in different scales using different robots are simulated using the developed method to illustrate its scalability. A numerical study evaluates the proposed method.

3.1 MH370 Search and Rescue Mission

In this section, the results of mission planning using the mission specifications (mission area, number of working robots and their battery capacities) are presented including the energy efficient trajectories for working robots and the placement of charging stations that minimize the energy and mission time under the mission constraints. To compare the performance of the presented method with alternate approaches, the

results of a greedy algorithm are also presented. The capability of the presented approach and architecture is used as a basis for analyzing the trade-off between the area of coverage, number of working robots, and the number of charging stations needed to support the mission. The lower and upper bound number of charging stations are obtained and an example trade-off study is presented for the example scenario.

A bounded mission area is considered with 20×23 km dimensions which is comparable to the map of the search area that the Bluefin-21 submarine operated as a working robot [40]. The goal is to search every kilometer square of an unstructured mission area of 208 km^2 using multiple working robots that can travel at the speed of 1 km/h and have a battery life of 22 hr with a capacity of 14.85 kWh. Working robots should be charged before reaching the critical battery level. In this map, illustrated in Fig. 3.1, environmental constraints are considered in the form of a high priority area (yellow area), two obstacle regions indicated by green areas, and the time-invariant and uniformly distributed current with the speed of 0.2 km/h. The mission area has 208 points, the unit distance (the distance between two closest mission points) is 1 km. Where applicable, weights from Eqn. 2.1 are picked as {2,8,5,1} and held fixed for generating results and evaluation.

We consider a case where three working robots are deployed to cover the 208 km^2 mission area illustrated in Fig. 3.1. During the mission, the working robots have to

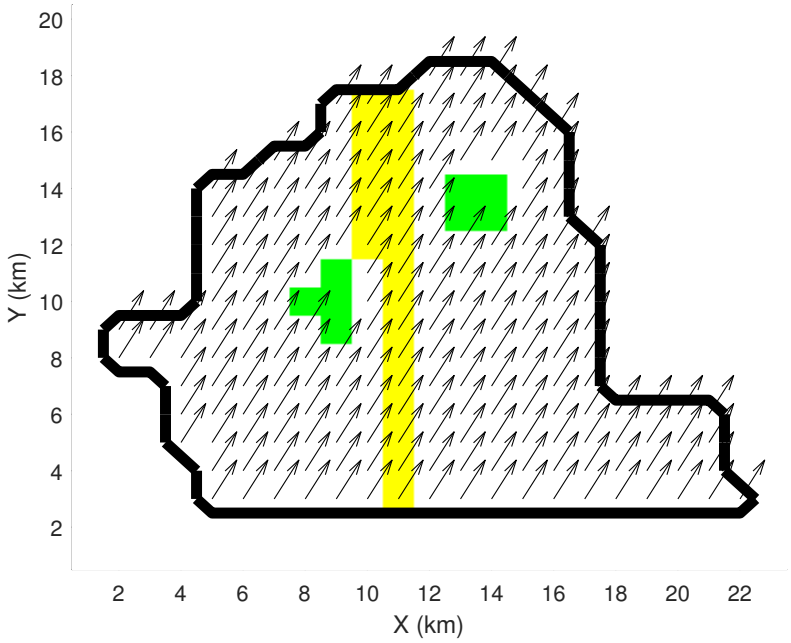

Figure 3.1: The mission area is discretized into mission points with the priority area (yellow), obstacle area (green), and time-invariant and uniformly distributed current (arrow).

reach the charging stations before their batteries are depleted. The charging time of the battery is not considered. There is no limit for the number of working robots that can be charged at one charging station at the same time. The results are first presented for a greedy algorithm compared to our algorithm to meet mission objectives and cover the mission area (Fig. 3.2 and 3.3), then more constraints are introduced to the simulation and their effects are demonstrated in Fig. 3.4. The GA results presented in this section are the results with the lowest cost out of 100 runs.

Working robot trajectories and charging station placement optimized by the proposed greedy algorithm is illustrated in Fig. 3.2 for the defined mission area without environmental constraints. The trajectories of the working robots are depicted by

different colored lines and the charging stations are represented by black squares. The travel distance for three working robots is 235.7 km in total and the mission completion time is 83.3 hr. Following the trajectories, the three working robots visit charging stations and get recharged eleven times.

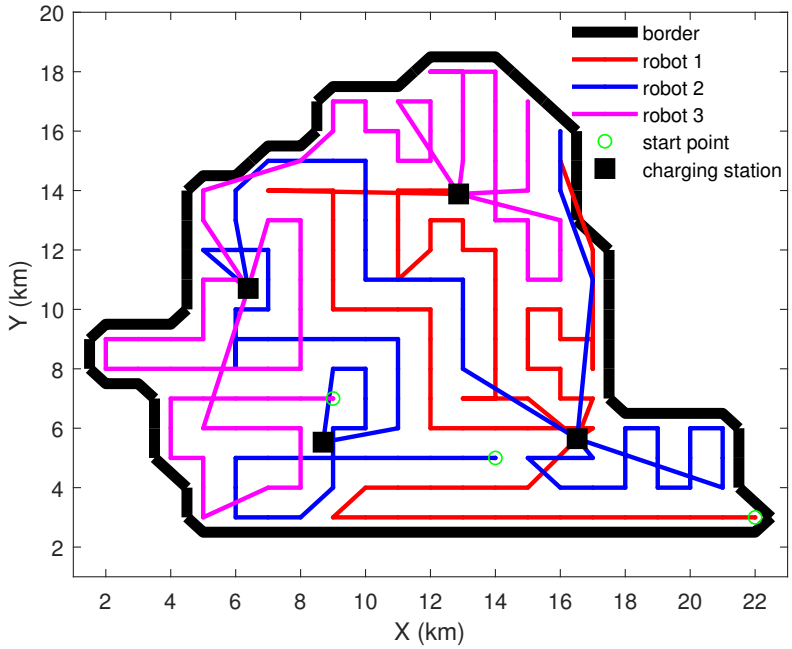

Figure 3.2: The greedy algorithm computes the trajectories of three working robots and the placement of four charging stations.

To compare with the greedy algorithm result, Fig. 3.3 shows the resulting planned trajectories of working robots and the placement of charging stations from the proposed mission planning method. The total travel distance of all working robots is 220.3 km, and the mission time is 78.2 hr. The working robots get recharged nine times in total. Compared to the greedy algorithm, using our method the total travel

distance and mission time is improved by 6.5% and 6.1% respectively. The greedy algorithm considering the environmental constraints is not studied, due to the difficulty of implementing all the constraints to a two-step optimization method. Specifically, the nearest neighbor algorithm is not effective in finding the trajectories of working robots with two objectives (minimizing the energy cost while visiting the high priority area early).

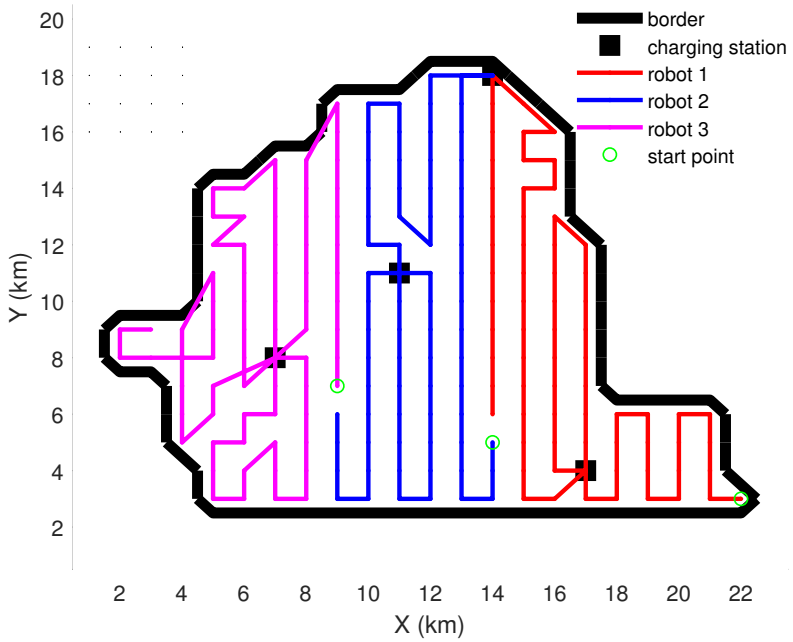

Figure 3.3: The proposed algorithm computes trajectories of three working robots and the placement of four charging stations.

The trajectories of three working robots covering the mission area in presence of environmental constraints using GA is illustrated in Fig. 3.4. The result shows that more charging stations (5 stations compared to 4 stations in previous case) are required when all constraints are considered including priority area, obstacle area, and

time-invariant and uniformly distributed current. The total distance traveled is 219.1 km with a mission completion time of 83.5 hr. With nine times of charging, three working robots spend 152.8 kWh in total. The relationship between the distance traveled by each robot and their energy expenditure is shown in Fig. 3.5. This plot shows the energy expenditure of each working robot on each battery life. The charging schedule and plan for visiting charging stations is decided by the algorithm, considering battery limitation and overall performance of robots. The figure also shows the effect of the current on the energy expenditure of working robots. The energy cost would have decreased linearly with the distance without the current effect. In these simulations, all the working robots have the same specifications (speed and battery life). However, the architecture is general and heterogeneous robots with a variety of specifications can be simulated using the same method.

We evaluate the presented approach and the effect of the number of agents on the results of planning using Monte Carlo simulation. The problem is solved 100 times for three charging stations and different number of working robots. Fig. 3.6 presents the average value and standard deviation of mission time, number of charging, travel distance, and percentage of feasible results (success rate) for three, five, seven, and nine working robots in Monte Carlo simulation.

The outcome of Monte Carlo simulation shows that the mission time decreases as the number of robots increases (Fig. 3.6(a)). This decrease is due to splitting the

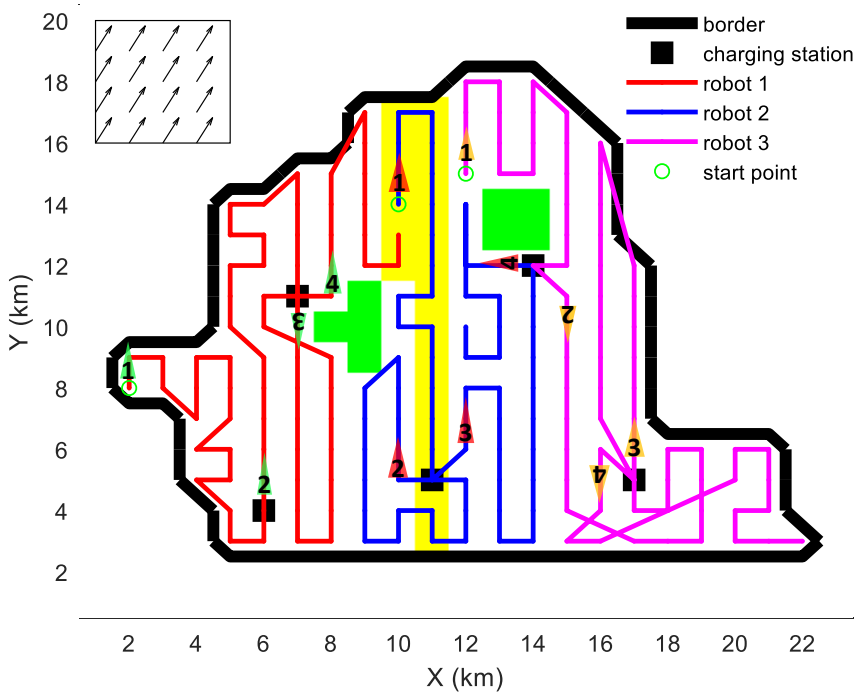

Figure 3.4: The proposed algorithm computes the trajectories of three working robots and the placement of five charging stations considering the environmental constraints. The order of each trajectory is numbered.

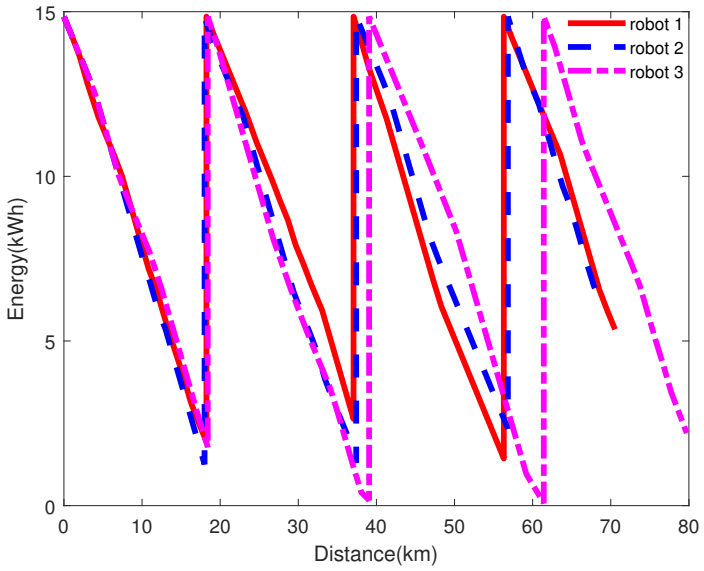

Figure 3.5: Relationship between distance traveled by each robot and energy spent on traveling.

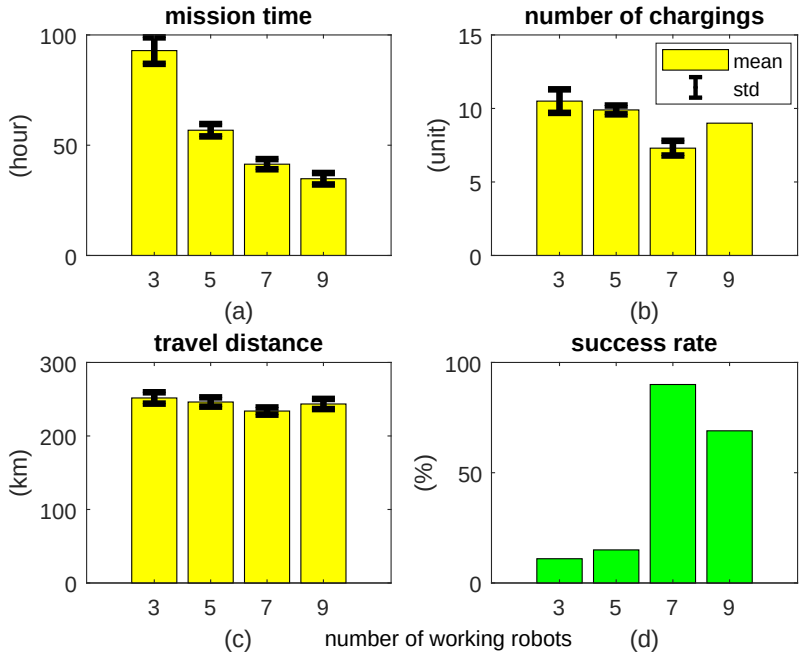

Figure 3.6: Monte Carlo simulation for finishing the mission using different number of working robots with three charging stations.

mission area between different robots. More robots can cover more mission points simultaneously and save time. The mean values of mission time for three, five, seven, and nine robots scenarios are 92.9, 56.8, 41.4, and 34.8 hr with the standard deviation of 6, 2.8, 2.3, and 2.6 hr.

Fig. 3.6(b) shows a decrease in number of charging required as the number of robots increases, because more energy is available to larger teams at the start of the mission. However, the nine robots scenario falls out of this pattern and has higher number of total charging compared to seven robots scenario. In nine robots case, each robot still needs to recharge once, however the robots have more unused energy left at the

end of mission, making the scenario less efficient from the number of charging point-of-view. This observation emphasizes on the importance of a planning approach that considers all aspects of the mission as a whole. In these simulations, each robot needs 3.5, 1.98, 1.04, and 1 battery charge on average respectively for three, five, seven, and nine robots. The total number of needed battery charge is obtained by multiplying those number by the number of robots, which results in 10.5, 9.9, 7.28, and 9 times with the standard deviation of 0.8, 0.3, 0.5 and 0 times.

Fig. 3.6(c) presents the total travel distance of working robots. The mean values of travel distance for three, five, seven, nine robots scenarios are 251.7, 246.2, 233.9, and 243.5 km with the standard deviation of 7.7, 6.3, 4.9, and 6.9 km. The travel distance depends on the size of the mission area and the recharging process which requires traveling to and from charging stations. The variation in the total travel distance reflects the pattern in Fig. 3.6(b).

Optimization solutions that do not exceed energy capacity (battery life) of working robots and maximum number of available charging stations are feasible results. Fig. 3.6(d) shows that when the resources are limited (three working robots and three charging stations), feasible solutions are rarely found. The success rate increased to 70% when we optimized the same mission for three working robots and seven charging stations instead of three. The success rate is closely dependent on the placement charging stations and charging schedule that has to be optimized. For

three, five, seven, and nine robots, the success rate are 11%, 15%, 90%, and 69%. The higher number of threshold positions in chromosome (Fig. 3.6(b)) results in a more complicated problem that reduces the success of optimization solutions.

To evaluate the impact of priority area consideration in the mission planning algorithm, we performed a numerical study. We compared a case where 21 mission points are marked as the high priority area with a probability of three times higher than the probability of the rest of the mission points (indicated by yellow area in Fig. 3.1) with the case of uniform distribution. In the first case when we are applying the higher probability value, the average time that all the high priority mission points are visited by a working robot is 34.9 hr with a standard deviation of 12.0 hr. Otherwise, the average time for the same points is 51.5 hr with a standard deviation of 22.7 hr. The results demonstrate the algorithm can address the objective of earlier coverage of high-priority areas.

Next, we demonstrate that the developed architecture will enable the user to a) study the impact of parameter changes, and b) develop a mission plan that ensures the robustness of robotic performance to accomplish area coverage missions limited by power and environmental constraints. The parameters include the number of charging stations (C) and working robots (W). Mission accomplishment is evaluated by the mission completion time, the total energy cost, and number of charging. The values of W and C can be given by users based on the available resources.

Table 3.1
Trade-off analysis for 3 working robots based on number of charging stations.

C	Time (hr)	Energy (kWh)	Number of charging	Scenario
1	invalid	invalid	invalid	
2	invalid	invalid	invalid	
3	85.6	167.9	9	min stations
4	84.9	162	9	
5	83.5	152.8	9	min energy

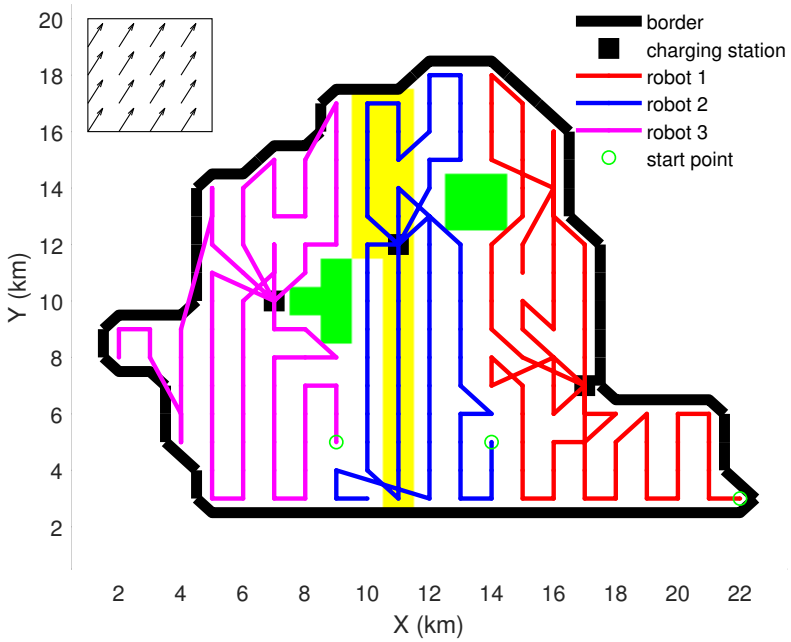

Figure 3.7: The genetic algorithm computes the trajectories of three working robots and the placement of least number of charging stations (three) considering the environmental constraints.

Table 3.1 presents the energy efficient mission planning results for three working robots ($W = 3$) and different numbers of charging stations. The table shows at least three charging stations are required to finish the mission. Having more than five stations will only reduce the mission time and energy slightly. Fig. 3.7 shows the

optimized trajectories with the least number of static chargers ($C = 3$). The mission completion time for this case is 85.6 hr during which the robots spent 167.9 kWh of energy on exploring. The total travel distance is 240.4 km with nine times of charging for three working robots. Figs. 3.4 and 3.7 illustrate the trajectories of three working robots and the placement of 5 and 3 charging stations based on the two mission objectives (least energy and least number of charging stations) considered here.

Table 3.2
Trade-off analysis results using 1, 3, and 5 working robots in minimum stations and minimized energy scenarios.

W	C	Time (hr)	Energy (kWh)	Number of charging	Scenario
1	4	254.1	171.5	11	min stations
	6	241	162.7	11	min energy
3	3	85.6	167.9	9	min stations
	5	83.5	152.8	9	min energy
5	3	51.4	164	10	min stations
	5	55.3	160.5	9	min energy

Table 3.2 presents an example of the trade-off analysis capability of the proposed approach. For each number of working robots (W), we find the minimum number of charging stations required to accomplish the mission objectives without violating the constraints. More charging stations are then added to conduct a cost-performance analysis and study the effect on improving the mission completion time and the energy spent.

The computational time is related to the population size of the GA. For example, we need to increase the population size to solve the problem that has more than

2000 mission points [40], and the computational time is increased from about 3 min to 2.5 hr each run. The computational time for the greedy algorithm is less than one second. The optimization is implemented in MATLAB on a desktop computer running a 64-bit Windows 10 Home operating system with a 3.20 GHz AMD A8-5500 APU processor and 10GB of RAM.

3.2 Yosemite National Park Search Mission

In a 2.5×2.5 km^2 area of the Yosemite National Park (Figure 3.8), four UAVs work collaboratively to take images and help the search and rescue of lost people. Having the information of the last location of the lost people, there is a certain area defined as high priority area.

The proposed method enables UAVs to search the priority area as early as possible while keeping the search time for the whole target area short. It is assumed that UAVs can fly at the speed of 36 km/h for 0.5 hour on a single battery charge. They need to land on one of the charging stations to be recharged before their batteries are completely depleted. The charging pads can be placed at assigned locations before the start of the mission. After each landing, there is a 5 min process before the UAV can take off and continue the mission. This example mission area contains tough terrain where placing the charging pads is not possible. Tough terrain areas are considered

Figure 3.8: The map of real mission area used in the simulation. Area by the creek is considered as high priority area. Tall mountain area is considered as obstacle area for placing charging stations.

as obstacles for the stations in the simulation.

The UAVs will maintain a 25 m height while following the optimized trajectories. The mounted cameras with a 90° Field of View (FOV) take pictures of a range of 50×50 m^2 areas. According to the camera range, the mission area uses a grid representation with a two-level resolution. The first level has 100 grids with the resolution of 250 m. Each grid in the first level has 25 smaller grids with the finer resolution of 50 m on second level.

The proposed method is applied to solve the planning problem of the search and rescue mission. The best result of GA out of 100 runs with the shortest mission time is presented. Then a numerical study is performed to evaluate the method. The weight vector for the GA cost function in Equation 2.1 is $\{1, 1, 3, 4\}$.

The optimized trajectories for the four UAVs are shown with different colored lines in Figure 3.9. The locations of charging stations are marked as black triangles that are only allowed to be placed outside of the tough terrain area, which is marked as yellow. The priority area where the UAVs will try to cover earlier than later is demonstrated as bright red region.

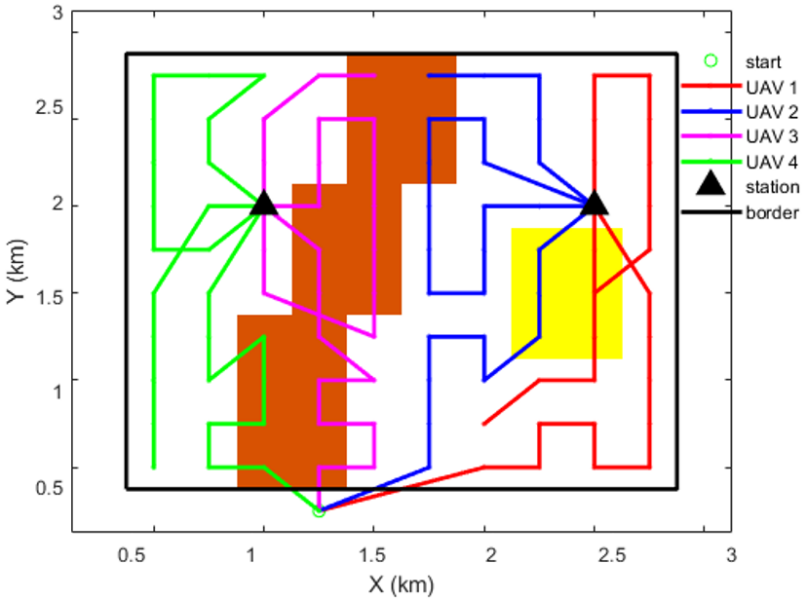

Figure 3.9: Level 1 trajectories for four UAVs with high priority area and obstacle area for charging stations. The resolution is 250 m.

The chosen trajectory pattern for each cell in level 2 is shown in Figure 3.10. This trajectory is one of the shortest trajectories that starts and ends at the same point. Therefore, the travel distance of this pattern in each cell is constant and equivalent to 1.27 km for a UAV following the trajectory pattern. Integrating the trajectory pattern in Figure 3.10 to the trajectories in Figure 3.9, the combined trajectories for the mission is shown in Figure 3.11. Starting from the start point at the same time,

the total travel distance for four UAVs is 158.74 km. The 20 priority cells are covered in 0.56 hours in average and the whole mission is completed in 1.36 hours.

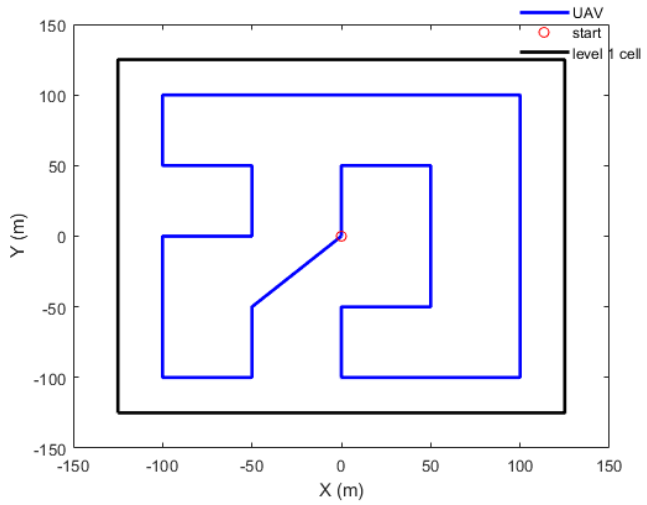

Figure 3.10: Level 2 trajectory pattern for UAVs. The resolution is 50 m.

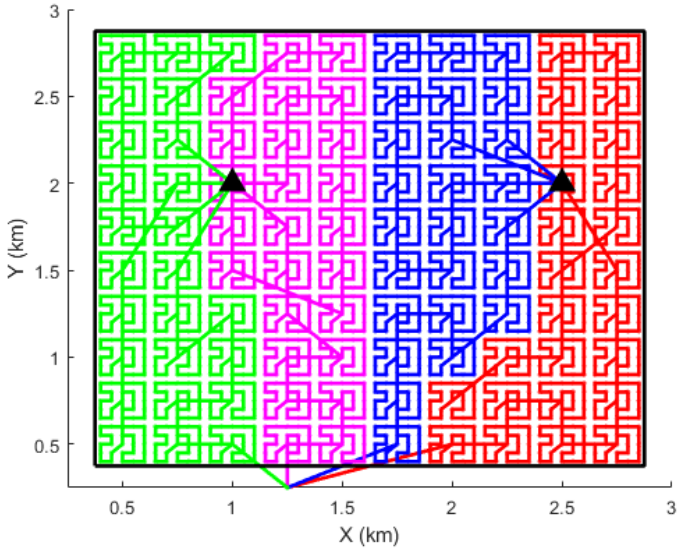

Figure 3.11: Trajectories for four UAVs combining level 1 trajectories (Figure3.10) and level 2 trajectory pattern (Figure3.9) at a resolution of 50 m.

Out of 100 results, the average total distance is 161.35 km with a standard deviation of 1.42 km. The average time to complete the mission is 1.39 hours with a standard

deviation of 0.02 hours. Among the 100 level 1 cells, the average time for covering 20 priority cells is 0.39 hours with a standard deviation of 0.24 hours.

To evaluate the performance of the algorithm and study the impact of priority area and obstacle area for stations, the GA simulation is run without considering those constraints for another 100 times. The results show that the average mission time remains at 1.39 hours with a standard deviation of 0.02 hours. The total distance traveled for UAVs is 161.91 km with a standard deviation of 5.58 km. The priority area is covered on average of 0.66 hours with a standard deviation of 0.17 hours. Figure 3.12 shows the comparison of the distribution of the visiting time of each cell in level 1, and the comparison of stations distribution by statistically analyzing two groups of 100 GA results.

It is observed that the mission map constraints (priority area and obstacles for charging stations) are successfully considered in planning the overall UAVs trajectories and placing charging stations. The proposed method is also capable of solving other situations. For example, area coverage problem with an unstructured mission area solved in [43]. The developed method formulates planning trajectories for multiple working agents, placing charging stations, and scheduling chargings simultaneously while accounting for environmental constraints. These multi-aspect considerations in the overall planning approach is missing in the existing methods.

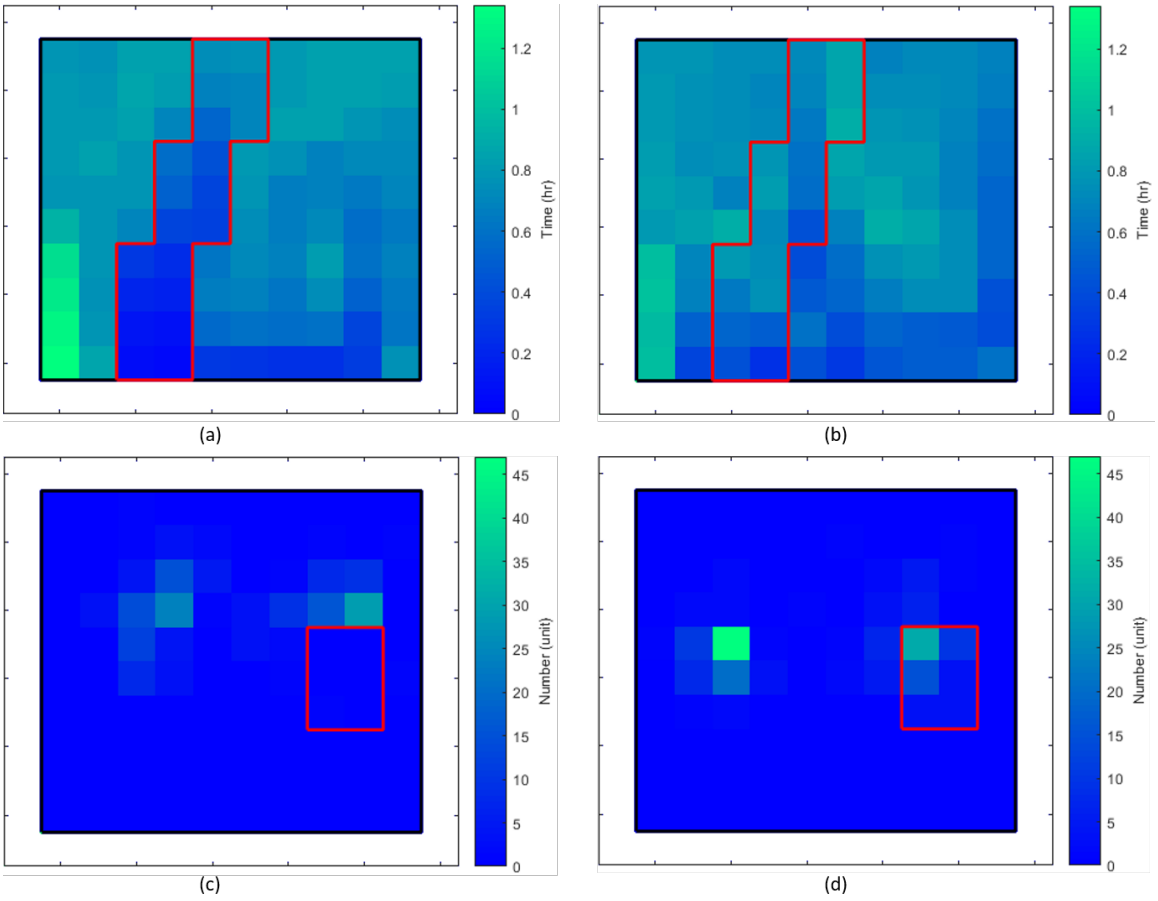

Figure 3.12: High priority area is within the red box in (a) and (b). These figures present the average visiting time distribution of each cell. Figure (a) considers priority area while (b) does not. Obstacle area for charging stations is within the red box in (c) and (d). These figures present the frequency of charging stations placement in each cell. Figure (c) considers the obstacle area for placing charging stations while (d) does not.

3.3 Oil Spill Detection Mission

The proposed method is applied to a sample scenario similar to the 1969 Santa Barbara oil spill accident (Fig. 3.13). The mission requires efficient survey of the area and collection of water samples for oil spill detection using multiple marine robots,

supported by charging stations. To illustrate the scalability of our approach, we show the implementations of two mission scenarios on different scales (Fig. 3.14). The mission configuration is presented in Table 3.3. We first deploy a team of ASVs to survey a large area to get an overview of the mission. Then a team of AUVs are deployed to the most suspicious area for in depth detection. Charging stations are placed to respond to the extended battery life and facilitate periodical inspections. The results presented in this section are the best results selected from 100 run of the GA algorithm. The weight vector for the GA cost function in Equation 2.1 is $\{\omega, 1, 1, 0\}$. The weight for priority area coverage is 0 since, this factor is not included in these mission scenarios. ω will change with different number of robots deployed and, its value for each scenarios is presented in Table 3.4.

Figure 3.13: Area of the oil spill accident near Santa Barbara in 1969 shown on Google map.

Multiple ASVs are deployed to survey a large area of 3100 km^2. This area is discretized into 124 cells. The ASVs need to visit every 25 km^2 of the mission area to collect

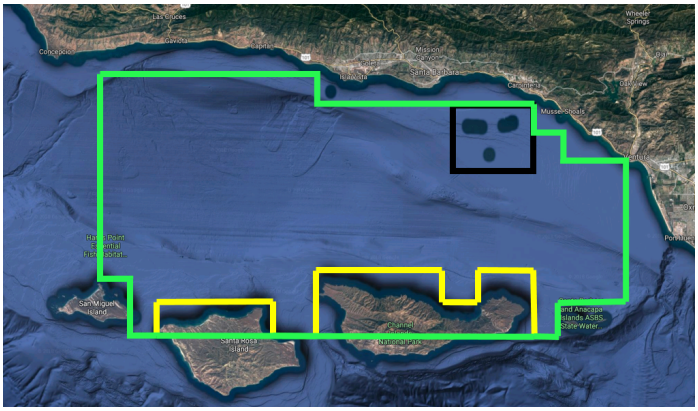

Figure 3.14: Mission areas near Santa Barbara indicated on Google map. Mission area for ASVs is inside the green box, and the mission area for AUVs is inside the black box. The yellow box indicates the obstacle areas.

Table 3.3
AUV and ASV configurations used in simulation

	Area km^2	Resolution km^2	Speed km/h	Battery life hour
AUV	169	1	3	10
ASV	3100	25	16	10

samples. Each ASV can operate at speed of 16 km/h for 10 hr. The battery charging time for ASVs is 10 hr. The results are presented in Fig. 3.15. For a bounded mission area (green line), we simulated the same coverage mission multiple times with different number ASVs. The mission area is an unstructured area with obstacles (yellow). To consider obstacles, a penalty is added to trajectories going across the obstacle area, so that the GA will eliminate those solutions from evolution. After deployment from the starting point (green circle), ASVs follow the optimized trajectories represented by colorful lines and go to the assigned charging station before depletion of their batteries. The locations of charging stations indicated by black triangles are also optimized. The total travel distance using one, two, and three ASVs with one charging station are

676 km, 679 km, and 668 km. The mission time for one, two, and three ASVs are 82 hr, 41 hr, and 24 hr respectively. The total number of charging attempts for one and two ASVs is 4 times, and is reduced to 3 times when using three ASVs.

The results show that increasing the number of ASVs has significant impact on the mission completion time but not on the travel distance. For example, the mission completion time is reduced to one day (24 hr) by using three ASVs in this scenario. Using the proposed method, a user can balance the required resources based on the mission specification and the desired performance.

After the large-scale survey mission using ASVs, multiple AUVs are deployed for a targeted area coverage mission. Considering an oil detection area of 13 by 13 km^2, the mission is simulated on 169 cells. Each cell has a length of 1 km, chosen based on the sensor range. AUVs have a speed of 3 km/h and a 10 hr battery life. It is assumed that AUV docking into the charging station and recharging the battery takes 10 hr.

The simulation results for this scenario are presented in Fig. 3.16, 3.17, and 3.18 for different number of AUVs. The optimized trajectories of AUVs are illustrated by colorful lines and location of charging station by black triangle. The total travel distance using one, three, and five AUVs with one charging station are 204 km, 200 km, and 199 km. The mission time for one, three, and five AUVs are 148 hr, 53 hr, and 35 hr respectively. The total number of charging attempts for one and three AUVs is 6 times, and for five AUVs is 5 times. We also simulated the mission with three AUVs

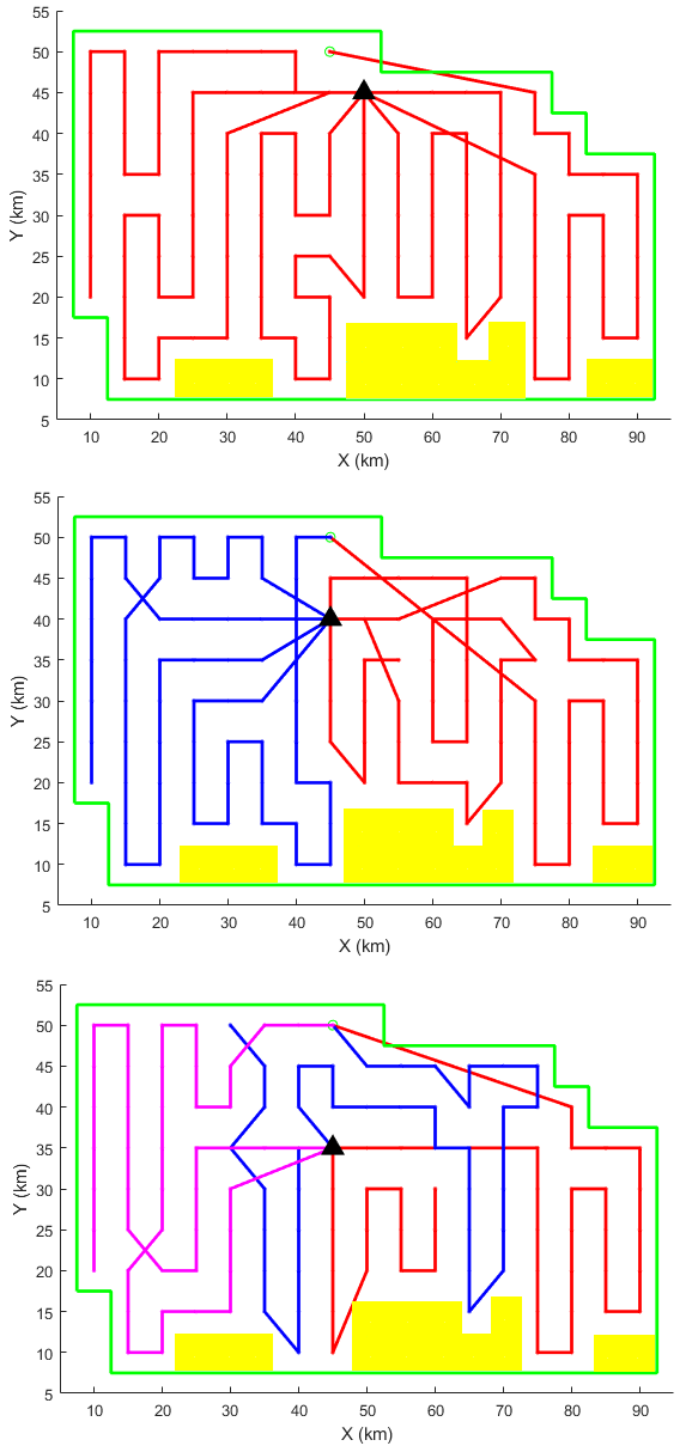

Figure 3.15: Simulation results of oil spill detection mission of 3100 km^2 area using one, two, and three ASVs and one charging station. Yellow areas are considered as obstacle areas. Green line is the boundary of mission area. Trajectories of ASVs are represented by colorful lines. Black triangle is the location of charging station.

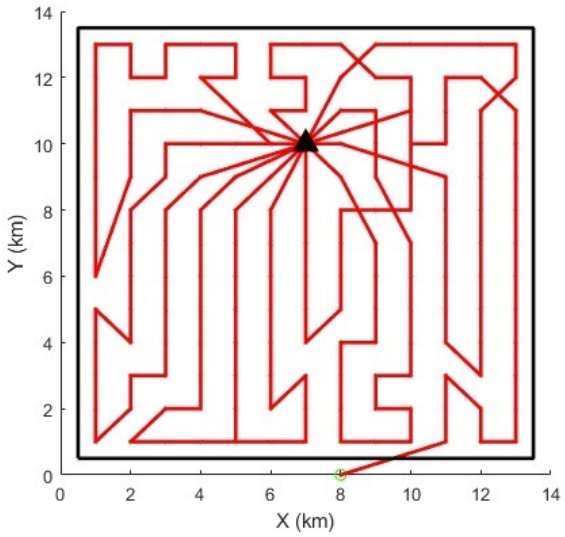

Figure 3.16: Simulation results of oil spill detection mission of 169 km^2 area using one AUV and one charging station. Black line is the boundary of mission area. Trajectories of AUVs are represented by colorful lines. Black triangle is the location of charging station.

and two charging stations. The result shows slight improvement on travel distance and mission time compared to using three AUVs and one charging station. Therefore for this scenario use of two charging stations is not justified considering the high cost of acquiring a charging station compared to an AUV. However, using multiple charging stations might be useful in other scenarios to meet mission specifications and respond to energy needs.

We performed a numerical study using Monte Carlo simulation by running the GA with the same configuration for each of the mission scenarios 100 times. The average value of total travel distance, mission time, number of charging attempts, and success rate are the evaluation criteria. Success rate is defined as finding a feasible solution with given number of charging stations. The results show it is harder to

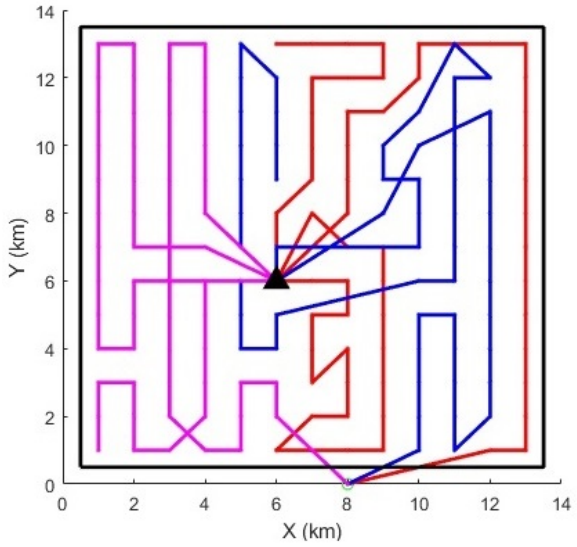

Figure 3.17: Simulation results of oil spill detection mission of 169 km^2 area using three AUVs and one charging station.

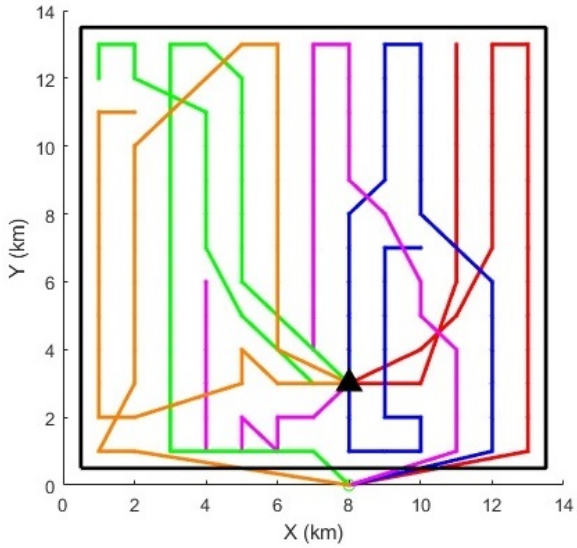

Figure 3.18: Simulation results of oil spill detection mission of 169 km^2 area using five AUVs and one charging station.

find feasible solutions with more charging attempts. In underwater applications, less charging attempts also lead to less failure due to the low reliability of underwater docking systems. The best results and mean values from Monte Carlo simulation are

Table 3.4
Best results of 100 run and average value of numerical study.

	Number of robot	Number of station	weight ω	Travel distance (km)		Mission time (hour)		Number of charging	Success rate
				Min	Mean	Min	Mean		
AUV	1	1	0.2	204	211	148	150	6	0.33
	3	1	0.2	200	210	53	55	6	0.38
	5	1	0.2	199	212	35	36	5	0.59
ASV	1	1	0.25	676	704	82	84	4	0.6
	2	1	0.25	679	703	41	43	4	0.61
	3	1	0.3	668	686	24	25	3	0.99

summarized in Table 3.4.

In this section, we implemented our method to specific mission scenarios to show its capabilities and test its performance. The simulation results demonstrate that the survey time for oil spill detection missions can be adjusted with deploying different number of marine robots. The results demonstrated that oil spill detection missions with two areas of 3100 km^2 and 169 km^2 can be completed within a week by deploying multiple marine robots with multiple charging if proper planning is performed.

Chapter 4

Multi-Robot Mission Planning with Mobile Energy Replenishment

To overcome energy limitations, existing solutions aim to automate the recharging process and increase robotic network performance via static charging stations [46, 47, 48]. This type of autonomous energy replenishment is appropriate for missions that have finite mission areas, such as surveillance and monitoring missions. However, the charging stations are still static in nature. This limits the total operational area of the vehicles by requiring them to expend energy on a return voyage to charge. Moreover, static charging stations are expensive to deploy and recover, limiting scalability for larger networks. In this chapter, we solve the long-term mission planning problem with the help of mobile charging stations. Figure 4.1 illustrates a

sample scenario where three Unmanned Ground Vehicles (UGVs) support four Unmanned Aerial Vehicles (UAVs) in mapping applications.

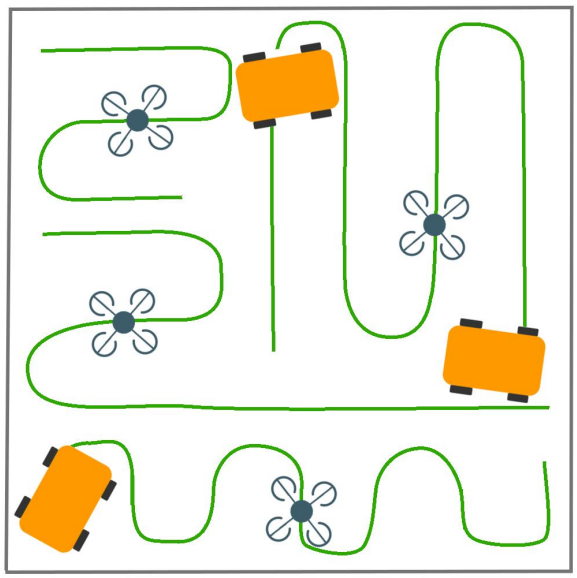

Figure 4.1: Illustration of the scenario showing four quadcopters (working robots) are deployed for a long-term mission with the support of three ground robots (mobile charging stations).

In Section 4.1, a rendezvous path planning method for mobile charging stations with pre-defined working robot trajectories is developed. The proposed method provides energy efficient rendezvous planning considering dynamic environmental disturbances and obstacles.

In Section 4.2, a mission planning method is proposed for both working robots and mobile charging stations under uncertain conditions. The method simultaneously generates trajectories of working robots and mobile charging stations with the capability of re-planning to account for the delay or failure of working robots.

4.1 Rendezvous Planning in Dynamic Environment

This section provides a rendezvous planning method which enables a team of working robots to finish a long-term mission with the support of a team of mobile charging stations. The scheduling and planning problem for mobile charging stations is solved by a graph transformation method considering dynamic currents.

4.1.1 Related Work

Rendezvous planning for recharging has been extensively studied in air to ground recharging scenarios [11, 33, 49]. Ground vehicles are usually used as energy carrying agents to rendezvous with and charge aerial vehicles periodically for long-term operation. Paths of aerial and ground vehicles are found with heuristic [33] and optimal [49] methods. Multiple ground robots rendezvous planning for recharging with pre-defined UAV trajectories are also solved with both heuristic and optimal methods [11]. However, none of these methods can account for environmental constraints (such as currents and obstacles) to be applicable to a variety of scenarios.

The planning and scheduling of robots require a precise understanding of the environment. This becomes more significant for underwater applications. The main forces to consider in the underwater domain are local currents which can affect a vehicle's heading or cause drift. The performance and path planning of AUVs under complex current conditions are studied extensively [50, 51, 52]. These methods fail to take energy limitation into account. Path planning for AUV rendezvous has also been developed while considering energy limitations and being aware of the dynamic currents and obstacles [53, 54]. However, neither methods are scalable for missions that have a large operational area or require quick completion because they only consider a single rendezvous.

Prior work on scheduling and planning persistent missions [11] is extended to underwater scenarios in this work by including real-world constraints for more practical mission planning. In [11], the path lengths of a team of mobile charging robots are optimized to rendezvous with the working robots and provide power on site. During rendezvous, the two vehicles will be close to each other for relative localization, allowing docking maneuver and energy transfer. The problem of finding a sequence of rendezvous locations is formulated and solved using an integer linear programming method and a graph transformation to a Traveling Salesman Problem. The approach of using a modified Noon-Bean transformation that can solve the Multiple Generalized Traveling Salesman Problem (MGTSP) for path planning of multiple charging robots is also developed. The results show that the transformation method provides

acceptable solutions for aerial and ground vehicle rendezvous planning with significant runtime savings.

Still missing, though, is a planning architecture that combines the promise of mobile charging stations with energy efficient collaborative robotic missions in presence of modeled dynamic disturbances and obstacles. The focus of this work is on addressing this shortcoming through integrating energy calculation of mobile chargers operating in a dynamic environment into the rendezvous planning method. A graph transformation method is proposed to minimize the energy cost of multiple mobile chargers for meeting working robots with pre-defined trajectories under the effect of dynamic disturbances. The problem is first formulated into a Multiple Generalized Traveling Salesman Problem (MGTSP), and then transformed to a Traveling Salesman Problem (TSP), which is solved using a Lin–Kernighan heuristic (LKH) solver.

4.1.2 Problem Statement

In this section, we define the problem of finding the energy efficient paths and recharge scheduling for a team of mobile chargers to rendezvous and charge a team of primary working robots. We make the following assumptions:

† The location of obstacles and a model of the dynamic currents in the environment are pre-known.

† The number of working robots and mobile chargers are chosen by the user.

† The working robots follow pre-defined trajectories during the mission and have the same configurations.

† All mobile chargers are homogeneous (same maximum speed and charge rate) with unlimited energy.

† The recharging process takes a fixed period of time for each rendezvous and is only allowed after the the battery level of an working robot drops below a threshold level.

Given a two-dimensional mission area where a team of W working robots are deployed, C mobile chargers need to rendezvous with and recharge the working robots within the charging window. The charging window is defined as the part of trajectories that the vehicles traverse with battery levels below the threshold value. The charging windows are then discretized into charging points $p_i(t)$, $i \in \{1, \ldots, W\}, t \in \mathbb{R}^+$. The mission area including obstacles and currents is also discretized into uniform cells, based on the fidelity of currents models. Mobile chargers need to rendezvous with working robots and charge them for a period of time Δt during visiting one point in each charging windows.

A directed graph $\mathbb{G}(V, A, \mathfrak{R}(x, y, t), \mathfrak{B}(x, y))$ is constructed, where V is the set of vertices, A is the set of edges, $\mathfrak{R}(x, y, t)$ is the model of currents, and $\mathfrak{B}(x, y)$ represents

the obstacle area, where $x, y \in \mathbb{R}$ are the coordinate of the cell and $t \in \mathbb{R}^+$ is the time. Vertices set V contains disjoint subsets $V_1, \ldots, V_l, l \in \mathbb{R}^+$. Each subset contains charging points in each charging window. Edges between two vertices are established with a direction from the first vertex to the second one. Edge costs associated with the edges are the energy costs of mobile chargers traveling from one vertex to the other, based on obstacle $\mathfrak{B}(x, y))$ and currents $\mathfrak{R}(x, y, t)$ models.

We define the multiple working robot rendezvous planning problem as finding a set of paths $\{P_1, \ldots, P_C\}$ of mobile chargers on graph $\mathbb{G}(V, A, \mathfrak{R}(x, y, t), \mathfrak{B}(x, y))$ collectively visiting all vertex subsets $V_1, \ldots, V_l$ (charging windows) once with minimum energy cost. The example of using two mobile chargers to support two AUVs is illustrated in Figure 4.2. It should be noted that the charging windows on a trajectory of an AUV are not pre-defined for the duration of the mission, but depends on the last rendezvous time and relies on the planned schedule.

4.1.3 Rendezvous and Recharging Planning Approach

To solve the proposed multiple working robot rendezvous planning problem with environmental constraints, which can be formulated as a Multiple Generalized Traveling Salesman Problem (MGTSP), we use a modified Noon-Bean transformation to covert MGTSP into a standard TSP. This method is described in details in [11].

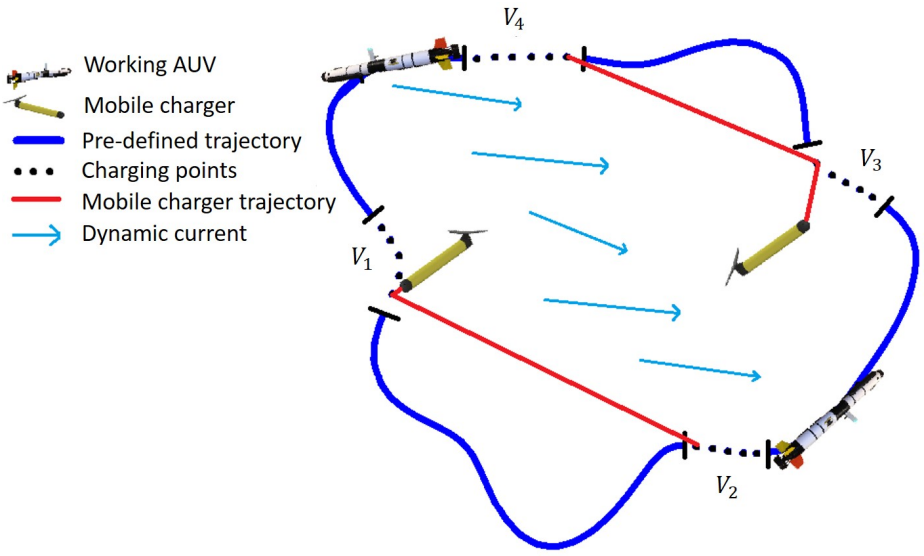

Figure 4.2: Problem illustration of finding paths and scheduling rendezvous for two underwater mobile charging stations to meet two AUVs twice, which follow the pre-defined trajectories of a surveillance mission under the effect of dynamic currents.

The MGTSP on graph $\mathbb{G}(V, A, \mathfrak{R}(x, y, t), \mathfrak{B}(x, y)$ is shown in Figure 4.3. V_0 is the vertex subset with initial positions of two mobile chargers v_0^1 and v_0^2. The goal is finding a set of paths starting from V_0 collectively visiting V_1, V_2, and V_3 exactly once with the lowest cost. A new graph $\mathbb{G}'(V', A', \mathfrak{R}(x, y, t), \mathfrak{B}(x, y)$ is used to represent the transformed TSP (Figure 4.4). V' has the same vertices as V in addition to vertices v'^3_0 and v'^4_0 indicating the finish vertices. Zero-cost edges from vertices in V'_1, V'_2, and V'_3 ending at v'^3_0 and v'^4_0 are added to the graph (dashed lines between subsets). The addition of v'^3_0 and v'^4_0 and their zero-cost edges allow constructing a large TSP path from multiple smaller paths that are concatenated together. In this example, two separate paths construct the total TSP path, one ending at v'^3_0 and the other at v'^4_0. The zero-cost edges are added within V'_0 to construct a directed cycle with

vertices ordered alternating between start and end vertices (e.g. $\{v'^1_0, v'^3_0, v'^2_0, v'^4_0\}$). Vertices in V'_1, V'_2, and V'_3 are connected together using zero-cost edges to form a directed single cycle. In V'_1, V'_2, and V'_3, the inter-set edges for each vertex are moved to the previous one in those cycles. For example, moved edges in Figure 4.3 and Figure 4.4 are indicated by the same color. Finally, except for edges ending at v'^3_0 and v'^4_0, penalty is added to all the edges between each subsets' vertices (bold edges in the figure) to encourage the path to go through the subset cycles before moving to another subset.

A Lin–Kernighan heuristic (LKH) solver is implemented to find a heuristic solution to the converted TSP problem on graph $\mathbb{G}'(V', A', \mathfrak{R}(x, y, t), \mathfrak{B}(x, y)$. LKH is a well-known heuristic solvers for TSP [55]. A feasible path can be found by a nearest-neighbor algorithm at the beginning. Then, LKH exchanges sub-paths by iterations. In each iteration, a sub-path visiting a chosen number of points will be replaced by a new sub-path with the same number of points visited. To improve the efficiency, the new sub-path needs to meet some criterion such as feasible and sequential check. LKH keeps finding shorter total paths until no improvement made by exchanging sub-paths. When the LKH solver stops, the output of the TSP solver is then translated to solution of the proposed problem.

To realize long-term autonomy, we provide our method to calculate the edge costs for A' considering environmental constraints. In the following subsections, we use a

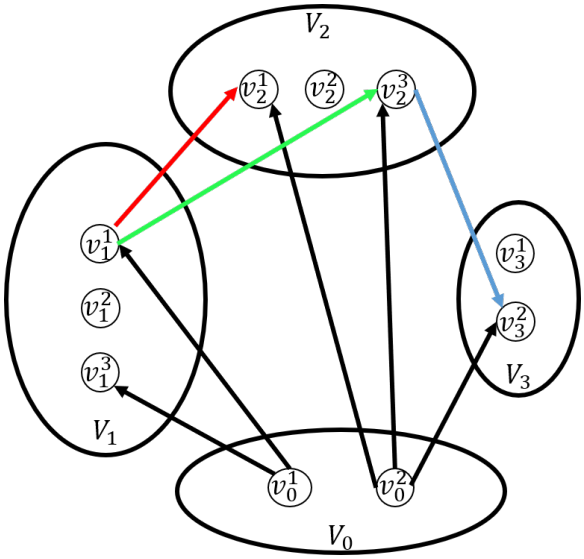

Figure 4.3: Modified Noon-Bean Transformation illustration using a scenario with three working robots and two mobile chargers. This figure shows the proposed MGTSP problem.

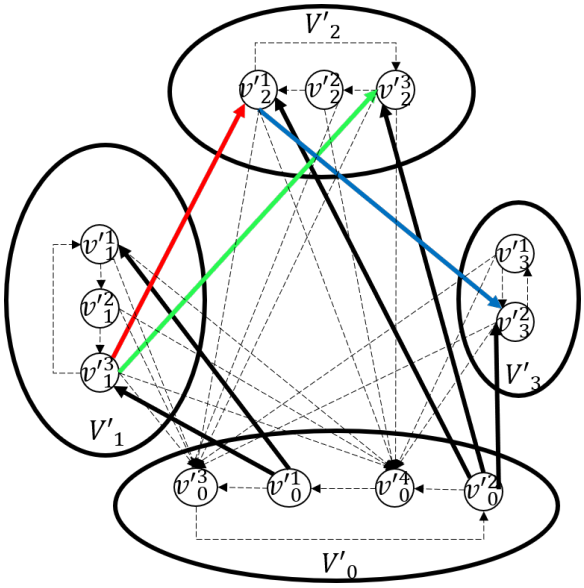

Figure 4.4: Transformed problem from Figure 4.3 using modified Noon-Bean Transformation. Dashed lines indicate created zero-cost edges. Moved edges are indicated by the same color. For clarity of the presentation, not all edges are shown in the figures.

grid-based energy cost evaluation to account for the effect of dynamic currents and obstacles (Section 4.1.3.1). A method to solve the multi-cycle recharging problem is also developed (Section 4.1.3.2).

4.1.3.1 Environmental Constraints Integration

For every edge in A', we find N cells along the edge to estimate the time required to travel through N cells by adding up the time for traveling through each cell, if none of them is an obstacle cell ($\mathfrak{B}(x, y)$), otherwise a large value is assigned to the energy cost as a penalty. We find the estimated travel energy $E_{m,n}$ for a mobile charger travels between two charging points $p_i(t_m)$ and $p_j(t_n)$ (where $i, j \in W$ and $m, n \in \mathbb{R}^+$) as shown in the Figure 4.5, where t_m and t_n are the time that working robots i and j arrive at those charging points.

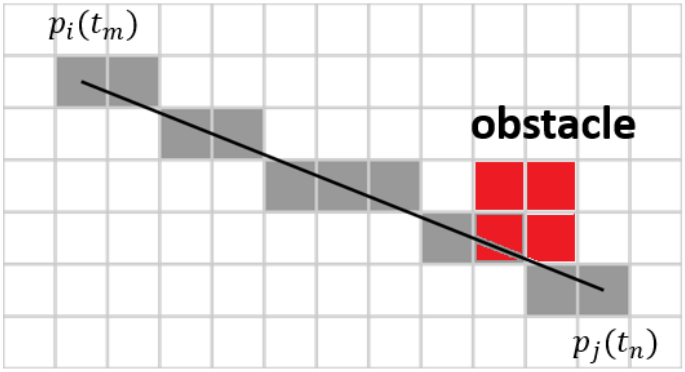

Figure 4.5: Illustration of calculating the edge cost of an edge between two vertices (charging points) and detecting obstacles.

For cell $k \in 1, \ldots, N$, we apply current model at the time of a mobile charger visiting

this cell, based on the mobile charger's speed. We calculate the global speed $\vec{v_k}$ of a mobile charger under the currents by calculating the water referenced velocity vector $\vec{S_c}$ and the current vector $\vec{v_k} = \vec{S_c} + \vec{R_k}$, where $\vec{R_k} = \mathfrak{R}(x, y, t_k)$, and t_k is the time spent visiting cell k. The velocity of a mobile charger under the current effect ($\|\vec{v_k}\|$) at time t_k can be calculated as

$$\|\vec{v_k}\| = \cos\alpha_1\|\vec{S_c}\| + \cos\alpha_2\|\vec{R_k}\|, \tag{4.1}$$

$$\alpha_1 = \arcsin(\sin\alpha_2\|\vec{R_k}\|/\|\vec{S_c}\|), \tag{4.2}$$

where α_1 is the angle between the desired travel direction $\vec{v_k}$ and the mobile charger's heading, and α_2 is the angle between the desired travel direction and the current's direction $\vec{R_k}$ as illustrated in Figure 4.6.

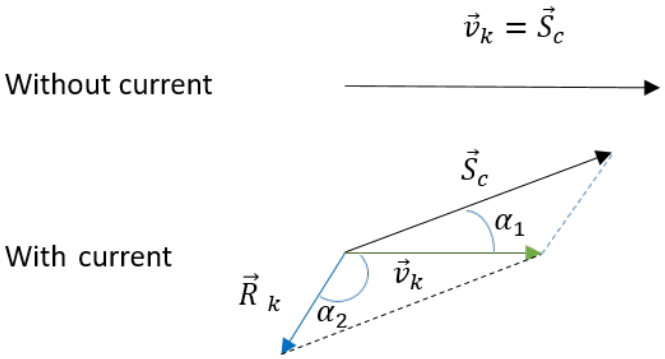

Figure 4.6: The current changes direction of the travel of a mobile charger. α_1 is the angle between the desired travel direction and the mobile charger's heading, and α_2 is the angle between the desired travel direction and the current.

The energy cost for this cell e_k, $k \in 1, \ldots, N$ is linear with the travel time of the

mobile charger,

$$e_k = \frac{c\,||p_i(t_m) - p_j(t_n)|\,|}{N\|\vec{v_k}\|}, \tag{4.3}$$

where c is a constant specifying the relation between operation time and consumed energy. The total energy cost for a mobile charger spent on traveling through the edge is $E_{m,n} = \sum_{k=1}^{N} e_k$.

An edge is feasible if the mobile charger has enough time to travel from $p_i(t_m)$ to $p_j(t_n)$ with the maximum velocity $\|\vec{S_c}\|$ considering the charging period Δt. A feasible edge meets the constraint

$$E_{m,n}/c \leq t_n - t_m - \Delta t, \tag{4.4}$$

otherwise, a large penalty will be added to the edge cost.

In addition to energy expenditure for traveling from one point to another, a mobile charging station also needs to spend energy to hold its position in currents while awaiting the working robot. After arriving at the designated rendezvous location, a mobile charging station needs to operate to the opposite direction of currents periodically to compensate the effect of currents. We call this station keeping energy, which is calculated as

$$F_{m,n} = \sum_{\tau=t_m+\Delta t+E_{m,n}/c}^{t_n} \|\vec{R_\tau}/\vec{S_c}\|. \tag{4.5}$$

Finally, we find the estimated energy cost $U_{m,n}$ for this edge by adding up all energy

cost

$$U_{m,n} = E_{m,n} + F_{m,n}.$$

With all the energy costs calculated for every edges, the LKH can be applied to the converted TSP in $\mathbb{G}'(V', A', \mathfrak{R}(x, y, t), \mathfrak{B}(x, y))$ to find the paths with the lowest energy cost.

4.1.3.2 Multi-cycle Recharging Scheduling

When the pre-defined trajectories for working robots require more than one recharge cycle, the upcoming charging windows depend on the the previous rendezvous time. In this section, we propose an iterative method to solve the multi-cycle recharging problem. The multi-cycle recharging problem can be solved by switching between a planning process and re-scheduling process multiple times. In the planning process, we solve the rendezvous planning problem with estimated charging windows. In the re-scheduling process, we re-define the charging windows based on optimized paths.

In the first iteration, we schedule all the charging windows of working robots required for the large-scale problem assuming every rendezvous happen in the middle of the charging windows. In the planning process, the rendezvous planning method in Section 4.1.3.1 is applied to find the paths and scheduling of mobile chargers visiting those charging windows. The result will be used in the scheduling process.

In the scheduling process, we find the real charging windows based on the rendezvous time, and verify them by checking if all the rendezvous are within the real charging windows. For each working robot, the rendezvous time are checked from the first one to the last one. Once a rendezvous is found out of the real charging window, we modify the estimated charging window and re-schedule the following estimated charging windows accordingly. The iterations will repeat until all the rendezvous are properly planned and scheduled for all working robots.

4.2 Mission Planning under Uncertainty

The overall robotic system can further improve its performance with the flexibility of optimizing working robot trajectories. This work shows the benefit of optimizing trajectories of working robots and mobile chargers simultaneously.

Unforeseen disturbances during a mission usually have negative impacts on the robot operations. This limitation becomes more critical in applications where robots have limited communication, such as underwater missions using AUVs. A mission planner that optimizes the overall robotic network and recharging system with the capability to re-plan during a mission is key to solving long-term mission planning problems including mission uncertainty.

4.2.1 Related Work

As explained in Section 2.1, long-term missions such as mapping, inspection, and monitoring missions can be considered as a Coverage Path Planning (CPP) problem. Traditional methods for CCP [18, 20, 22, 56] can optimize path length of working robots. Although mission efficiency is improved, these methods fail to consider any energy limitations of robots, which limits their applications. Taking energy limitations as constraints, several methods manage to plan mission scenarios efficiently in a limited area [57, 58, 59]. However, without overcoming the energy limitation, these methods are not scalable and implementable to a wide range of long-term missions.

To address the energy limitation of working robots, multi-robot energy cycling utilizing mobile charging stations has been studied extensively [33, 49, 60, 61]. An autonomous mobile charging station for multi-robot applications has been proposed [61]. Paths and a charging schedule utilizing mobile chargers were found by optimal [49] and heuristic [33, 60] algorithms. However, these methods do not account for disturbances and uncertainty during the mission.

Previous knowledge of the environment including obstacles [15], disturbance [37, 38], and adversary areas [14] has been successfully considered in pre-planing methods. Taking unforeseen conditions into account can further improve long-term mission

robustness [62]. Still missing is an approach that plans the working robot and mobile charger trajectories simultaneously in the presence of a challenging environment.

In this section, a mission planning approach is developed for a multi-robot area coverage mission to be undertaken by a team of primary working robots and a collaborating team of mobile chargers. A Genetic Algorithm (GA) based approach is introduced with the capability of re-planning to compensate for mission uncertainty.

4.2.2 Problem Statement

Consider a mission where multiple working robots cover a large area, the problem is to find the optimized working robot trajectories to cover the whole mission area in the presence of the uncertainty, with the support of a team of mobile chargers. We construct a 2D grid map to represent the mission area. The constructed map has N uniform cells. Each cell needs to be visited by one of the working robots at least once to complete the mission. The center of the cells are defined as mission points. We assume that the disturbances such as currents will not remove working robots from their assigned trajectories, but will delay or stop working robot operations. Disturbances do not impact the mobile chargers.

The number of working robots is represented by W and the number of mobile chargers is represented by C. The working robots can operate G hours at a speed of V.

We assume that all working robots have the same energy capacity and maximum velocity, and G is smaller than the actual battery capacity to consider a safety level. Before a working robot runs out of energy, it needs to be recharged by docking into a mobile charger. Mobile chargers have a maximum speed of V_c with unlimited energy. Recharging procedures take a period of time ΔT for each rendezvous. Each mobile charger can charge only one working robot at a time.

For a working robot indexed by w, its mission time T_w is the summation of the trajectory-following time, time of waiting mobile chargers, and total charging time. The trajectory-following time can be calculated by its total travel distance and speed (V). The waiting time is considered as a mobile charger reaches the designed rendezvous locations later than the working robot, which can be calculated by the rendezvous times, the distance between rendezvous locations and the speed limit of a mobile charger (V_c). The total charging time is calculated by charging period (ΔT) multiplied by the number of charging processes. The mission completion time is represented as $T = max(\{T_1 \dots T_W\})$.

The mission planning problem can be defined as finding and updating the trajectories of working robots and mobile chargers considering the energy limitation of working robots, so that the total mission completion time (T) is minimized. During the mission, the operation of a working robot can be delayed by unpredicted environmental disturbances, which may increase the mission completion time. The mission operator

can re-plan trajectories by running optimization again based on updated information.

4.2.3 GA Based Mission Planning Approach

Given mission specifications and available resources, the mission planning problem is solved by a GA based method. The proposed GA uses discretized mission points, number of working robots and mobile chargers, and robot configurations (including starting locations, battery capacity, maximum speed, and charging period) as inputs to find trajectories of working robots and mobile chargers. The proposed optimization process can be repeated multiple times during a mission to compensate for errors caused by environmental uncertainty. In each repeated optimization process the inputs to the GA (number of working robots, starting locations and times, uncovered mission points) will be updated.

4.2.3.1 Pre-plan Genetic Algorithm

An illustration of GA design is presented in Figure 4.7. In the initialization process, the initial population is randomly generated. We use a fixed length decimal chromosome to represent N mission points as N genes. The order of the genes in the chromosome represents the trajectories of working robots. Each chromosome is evenly divided by the number of working robots to uniformly distribute workload to

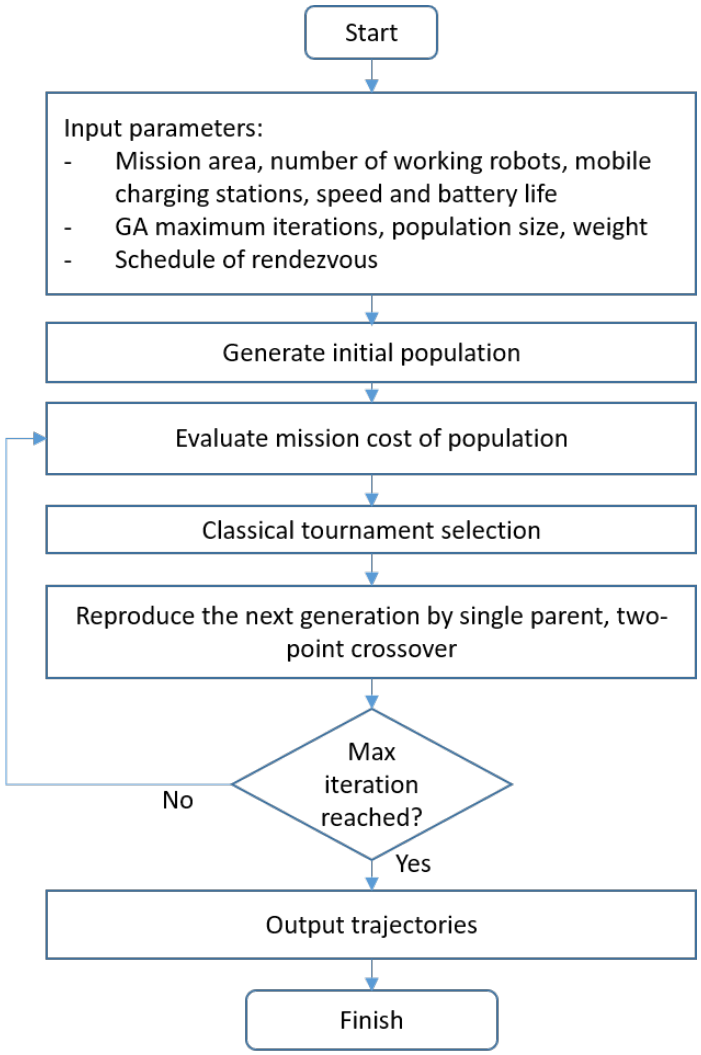

Figure 4.7: The steps of GA solving the mission planning problem by finding trajectories of working robots and mobile chargers.

each working robot (Figure 4.8). The chromosome distribution does not change with iterations of the GA.

In the evaluation process, we calculate the cost of each chromosome. The objective is to minimize the total mission time T considering the energy limitation of the working robots. Therefore, the cost function is designed to minimize the travel time of working

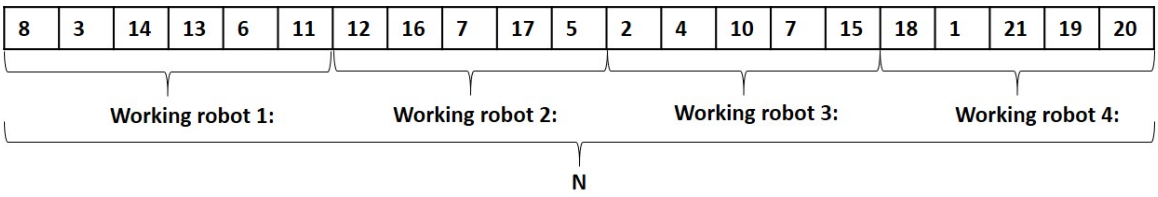

Figure 4.8: Each chromosome represents trajectories of all working robots.

robots, and penalize the late arrival of mobile chargers. Minimizing the travel time reduces total charging time because less travel time leads to less rendezvous.

The total travel time of working robots, as well as rendezvous locations and time can be obtained by analyzing the chromosome. The total travel time can be used to evaluate the mission cost, and rendezvous locations can be used to satisfy the energy limitation constraint and find mobile charger trajectories. For each segment of a chromosome that represents a working robot trajectory, we analyze the trajectory based on the order of genes. We keep track of the remaining battery level by calculating the travel time from one mission point to the next one. If traveling to the next mission point requires the remaining battery level to drop below the minimum level, then the current mission point of this working robot is marked as a rendezvous location, and its remaining battery level is reset to G.

All rendezvous locations is assigned to mobile chargers. Since each mobile charger can only charge one working robot at a time, it becomes unavailable for a period of time (ΔT) after meeting with a working robot. Having all rendezvous locations and times, each rendezvous is scheduled to the next available mobile charger. If more

than one mobile charger is available, the closer one is assigned. The mobile charger trajectories associated to each chromosome are obtained from this process.

A weighted sum approach converts the multi-objective optimization problem into a single objective optimization problem to calculate the cost of each chromosome. The cost function is expressed as

$$\text{Cost} = \omega \sum_{w=1}^{W} L_w + \sum_{c=1}^{C} Y_c \tag{4.6}$$

where L_w denotes the total travel time of a working robot indexed by w, the second term Y_c penalizes the late arrival of a mobile charger indexed by c, and ω is a weight. The weight ω is decided by the speed of the mobile chargers (V_c). For example, the mission planner can use a smaller ω to encourage the algorithm to reduce larger penalty caused by the mobile chargers with a lower speed limit.

We denote the number of rendezvous for mobile chargers c as n_c. The penalty for late arrival can be calculated as

$$Y_c = \sum_{i=1}^{n_c} K_i / n_c,$$

where K_i is the late time of the ith rendezvous calculated by maximum speed of mobile chargers V_c.The solution of mobile charger trajectories is coupled with the trajectories of working robots. Long working robot trajectories need more meetings

with mobile chargers, which results in long mobile charger trajectories. To decouple the two sub-objectives, Y_c is normalized by the number of rendezvous n_c for mobile charger c. This normalization will facilitate the GA to get out of a local optima.

Taking advantage of the even distribution of mission area, the minimization of the total travel time of working robots will lead to the minimization of the maximum travel time. Minimization of total travel time provides a better direction for GA evolution, compared to minimizing the mission completion time (T) directly. Only the working robot with the longest mission time will change the cost, if T is the cost of the chromosome.

After calculating the costs, all chromosomes are randomly grouped. Each group has four chromosomes. A tournament selection is used to select the best chromosomes from chromosome groups as parent chromosomes of the next generation. A single parent crossover is used to prevent duplicated genes (Figure 4.9) in the crossover process. The child chromosomes are obtained by performing two points flip, swap, and slide to the selected parent chromosomes [1]. The crossover grows the number of chromosomes four times, keeping the size of the population constant from one iteration to the next.

The iterations stop when the algorithm meets the maximum number of iterations. The chromosome representing the trajectories of working robots and mobile chargers with the lowest cost is the output of the algorithm.

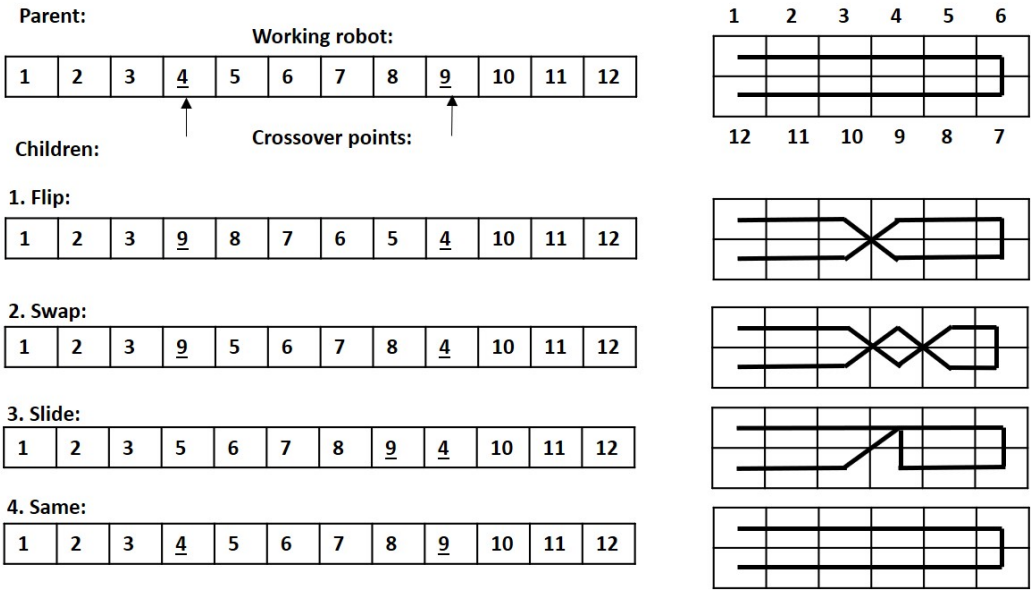

Figure 4.9: The population reproduction uses a single parent two-point crossover process [1]. The illustrations of the decoding of each offspring are shown on the right.

4.2.3.2 Re-plan Genetic Algorithm

In the event that a working robot encounters a disturbance in operation, the mission completion time may be delayed. In the worst case scenario, the mission can become infeasible due to the failure of a working robot. To reduce the impact of disturbances, the optimization can be conducted again to find new feasible trajectories for working robots and mobile chargers. To re-plan, the GA updates the number of available working robots with their current battery levels, starting locations and times of all robots, and uncovered mission points in the initialization process. The updated information is used to change the length of chromosomes and generate new workload distribution for working robots. The length of the chromosome is shortened to the

number of uncovered mission points. The working robots with higher battery level is assigned to more mission points by having more genes in the chromosome. The re-plan GA evaluates the mission cost in the evaluation process and chooses the most fit chromosomes to produce the next generation, the same as the pre-plan GA. The re-plan GA has a smaller population size and number of iterations based on size of the remaining mission area.

Chapter 5

Mission Planning Applications with Mobile Energy Replenishment

The developed mission planning methods utilizing mobile charging stations in Chapter 4 are implemented into two real-world underwater applications to show their capabilities, especially in handling dynamic environmental constraints. Numerical studies with robot configurations are conducted to measure the performance of methods.

In Section 5.1, multiple coverage mission scenarios in Lake Michigan are simulated to analyze the efficiency of rendezvous planning in presence of obstacles and dynamic currents. Also, the capability of the method in planning many consecutive charging is investigated. The method of planning mobile charger trajectories is then compared

to previous work through statistical analysis.

In Section 5.2, a long-term area coverage mission in Portage Lake using multiple robots and mobile charging stations is simulated under unforeseen environmental disturbances. Given the mission and robot specification, the designed algorithm minimizes the mission completion time by optimizing trajectories of working robots and mobile charging stations. GA is also used to re-plan the mission in case of the delay and failure of the working robots during the mission.

5.1 Lake Michigan Area Coverage Mission

In this section, the missions of mobile power delivery vehicles to extend AUVs' operation in a dynamic underwater environment are simulated to validate the algorithms developed in Section 4.1. The missions are performed by AUVs with the support of ASVs as mobile chargers in a 40 km by 40 km area in Lake Michigan. Current models built from real gathered data provide information on current direction and magnitude in mission area during a one-week time period, with spatial resolution of 1 km and temporal resolution of 1 hour (Figure 5.1). Based on the prior knowledge, the mission area contains obstacle areas. In this work, we assume that only ASVs need to avoid obstacles. For example, obstacles can be buoys and crowded area with boat traffic, which only affects surface vehicles.

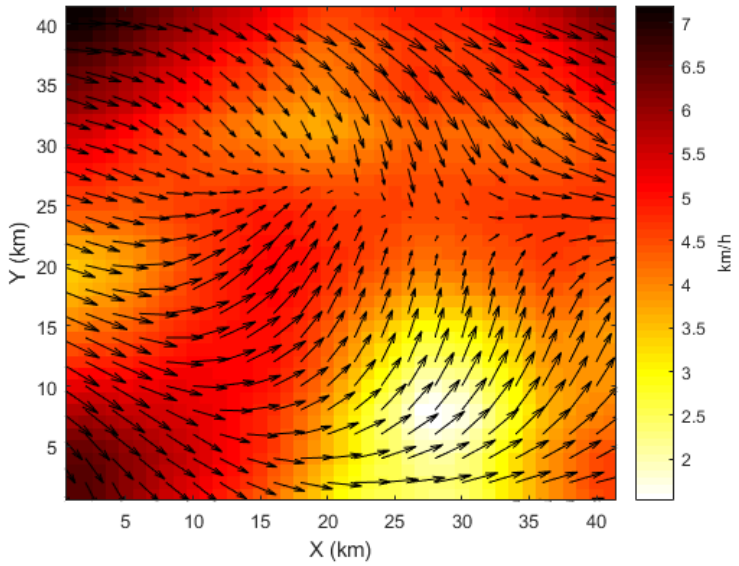

Figure 5.1: Illustration of a current model in the mission area. The directions of arrows indicate the directions of currents, and the magnitudes of the currents are represented by the heat map. The resolution of the model is reduced for clarity, and current magnitudes are magnified 13 times in simulation.

Four AUVs collectively following the pre-defined trajectories are simulated to perform a coverage mission. In these simulations, AUVs have a 15 hr endurance at a speed of 6 km/h. The charging window is configured as 0-30% battery level. The ASVs has a speed of 4 km/h. Each rendezvous takes 1 hour. Using four AUVs, we first present the result for a sample scenario with dynamic currents and obstacles. Next, we apply the method for planning a scenario that requires large number of chargings to accomplish the mission. Finally, the performance of the proposed method is statistically evaluated by simulating scenarios under different current conditions. We compare the statistical results of our proposed method that works based on energy minimization with the results calculated for the distance minimization method that

does not consider currents in planning [11].

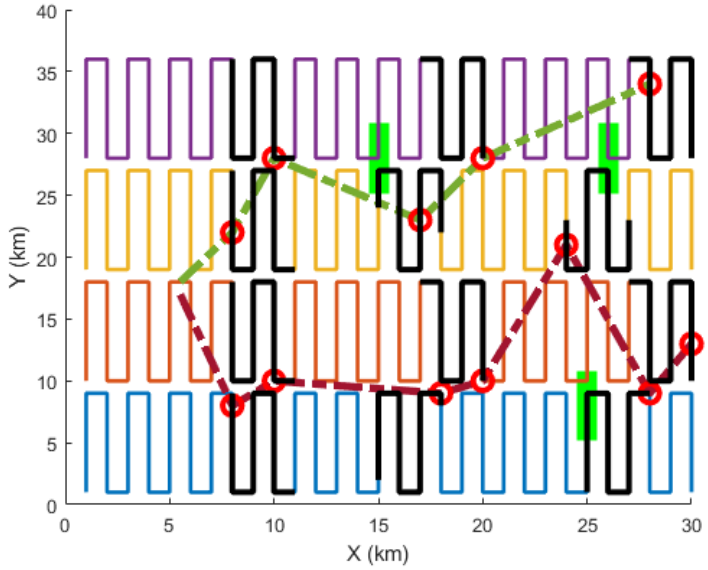

Figure 5.2: Rendezvous planning for energy minimization with four AUVs and two ASVs considering the effect of dynamic currents and obstacle areas.

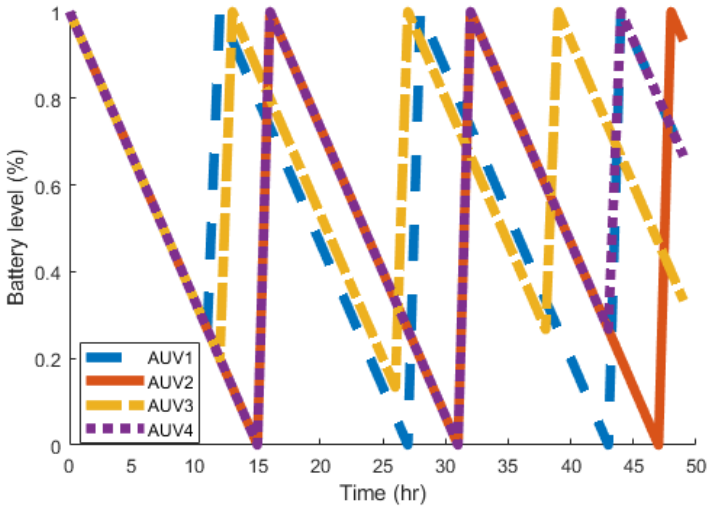

Figure 5.3: Battery level of AUVs during the mission in Figure 5.2.

Figure 5.2 illustrates an example mission scenario and the planned trajectories for

energy delivery. The AUV trajectories are pre-defined as lawn mower paths, represented by colored lines. The trajectories generated by the proposed method for ASVs are represented by colored dashed lines. The optimized rendezvous locations are shown as red circles. The charging windows are indicated by black lines portions along AUV trajectories. Obstacle areas are shown as green rectangular in Figure 5.2. Since the energy cost is linearly proportional with the operational time of ASVs, the energy costs presented in this section are in the format of operational time. The simulation results show that the two ASVs are required to spend a total time of 54.4 hr for traveling and station keeping, 25.2 hr and 29.2 hr respectively. The result shows that the method successfully visited all the AUVs during their charging windows by overcoming the obstacles and dynamic currents in the environment (Figure 5.3). The total mission time is 49 hr to finish covering 1080 km^2 area in this simulation.

In the simulated scenario presented in Figure 5.2, each AUV needs to rendezvous with a mobile charging station for recharging three times. To demonstrate that our method is able to plan more recharging cycles, we also perform another simulation study with same number of AUVs and ASVs having ten rendezvous considering a larger area coverage mission. The mission is planned without considering any currents and obstacles. The result shows the total mission time is 160 hr to cover an area of 3600 km^2. All the rendezvous are planned within the charging window, and the AUV gets recharged at 6.8% battery level on average with a standard deviation of 9%.

Table 5.1
Comparison between distance and energy minimization using slow ASVs

Mission objective	Energy cost (hr)		Mission time (hr)	Success rate
	Travel	Station keeping		
Distance	20.1	32.1	49	40%
Energy	19.8	27.4	49	100%

For statistical analysis, we simulate the same mission area as in Figure 5.2 with ten different current models. The currents have a maximum magnitude of 3.6 km/h, which makes the mission challenging for ASVs (4 km/h speed). Using the same pre-defined trajectories for the four AUVs, we generate the paths of the two ASVs using two approaches. One is the energy optimization method proposed in this work, and the other one is a distance minimization considered in [11]. We compare the two approaches by analyzing the energy cost of two ASVs under dynamic currents and the success rate. The success rate is measured by whether or not the AUV can get recharged during their charging windows.

The results show that compared to the distance minimization, the proposed method can save the total energy cost of the mission by about 10% (Table 5.1). The mission has a higher chance to succeed if the proposed energy optimization method is used. This improvement is the result of integrating environmental conditions into planning with energy requirement consideration.

To further evaluate our method and demonstrate the effectiveness of adapting to different types of vehicles, another evaluation is performed using different charging

Table 5.2
Comparison between distance and energy minimization using fast ASVs

Mission objective	Energy cost (hr)		Mission time (hr)	Success rate
	Travel	Station keeping		
Distance	36.3	102.5	49	100%
Energy	56.3	60	49	100%

agents specifications (Table 5.2). In this case, ASVs with higher speed of 10 km/h are considered where the currents have less impact. Faster ASVs spend higher energy cost by a factor of 6.25. The results show that both approaches can successfully plan the mission. Using the proposed method, the total energy cost is reduced by about 16% compared to distance minimization. The travel energy cost for distance minimization is less than the proposed method, because it ignores the station keeping energy cost.

The results presented in this section suggest that the consideration of dynamic currents and directly optimizing the energy cost can significantly improve mission efficiency and feasibility. The proposed method is scalable for multiple number of working vehicles, ASVs, and multiple recharging cycles. It is also independent from the characteristics of the performing vehicles.

The simulations in this section were performed in MATLAB environment on a desktop computer running a 64-bit Windows 10 Home operating system with a 3.20 GHz AMD A8-5500 APU processor and 10 GB of RAM. The computational time of the proposed algorithm is related to the consideration of currents and number of charging

points. The computational time of energy minimization is 19.2 seconds in the sample scenario and statistical simulations, where a total of 360 charging points are considered. Without considering currents, the computational time is 4.4 seconds for 360 charging points, and 51.2 seconds for 1200 charging points. The proposed method is computationally efficient enough to run constantly during the mission and keep the mission plan updated with the newest current models to further improve the performance of the network.

5.2 Area Coverage Mission in Portage Lake with Uncertainty

In this section, we demonstrate performance of the presented method in Section 4.2 using an underwater coverage mission scenario in a large area of Portage Lake. AUVs are deployed as working robots with the support of ASVs as mobile charging stations in a square mission area of 14×14 km^2. During the mission, ASVs carry batteries to the rendezvous locations, where the AUVs will dock and replace their batteries. We apply the proposed method to minimize mission completion time. Its capability of handling unforeseen environmental disturbances is also illustrated. The effectiveness of the proposed method is evaluated by numerical studies.

We use 1×1 km^2 uniform cells to grid the mission area. The cells need to be visited

by one of the AUVs at least once. The AUVs deployed in the mission can travel at the maximum speed of 3 km/h for 10 hours. Before the AUVs run out of battery, they need to meet one of ASVs and get recharged. The ASVs have a speed limit of 2 km/h. For each rendezvous, the battery swapping process takes 2 hours. We can easily calculate that an AUV following traditional lawn-mower trajectory needs to travel 196 km in 77.3 hours with 6 times recharging.

In this mission, three AUVs are deployed with different battery levels (full, two thirds, and one third of battery) to avoid running out of battery at the same time. At the first rendezvous, they are recharged to full battery level. Two ASVs are used to rendezvous with the next AUV that needs to recharge.

We first present trajectories of AUVs and ASVs optimized by the pre-plan GA for the whole mission area. Environmental disturbances such as delays in trajectory-following and complete failure are then applied to the AUVs. When the mission completion time is significantly delayed, the re-plan GA is used for the uncovered mission area to reduce the impact of environmental disturbances on overall mission performance.

The GA is configured as having a maximum iteration of 1200 with the population size of 1200. The weight ω in Equation 4.6 is 0.8. The pre-plan GA is repeated 100 times with the same inputs and GA configurations. The best pre-plan GA result for completing the coverage mission is presented in Figure 5.4. The operational time of three AUVs in Figure 5.4 is shown by the bars in Figure 5.5.

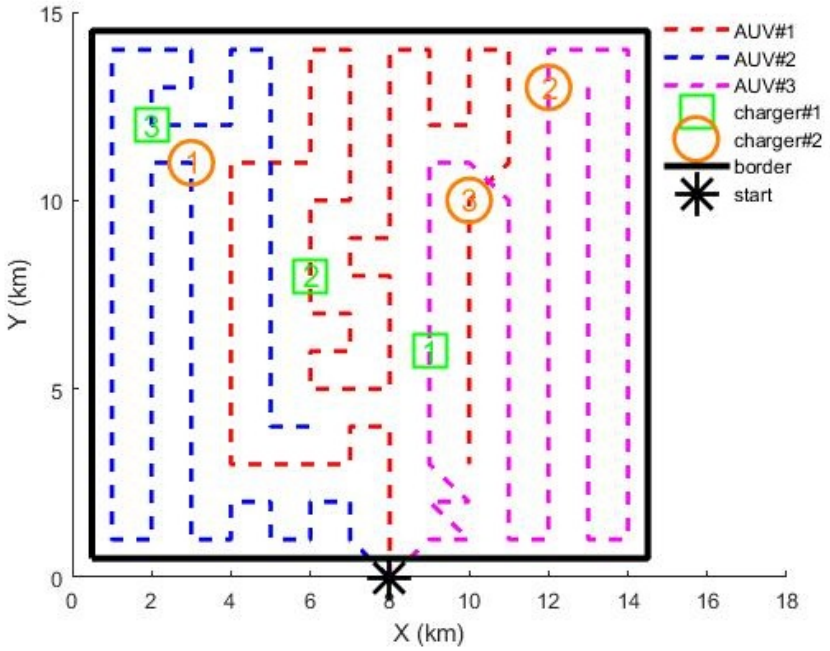

Figure 5.4: Pre-plan GA optimizes trajectories of three AUVs and two ASVs to cover the whole mission area.

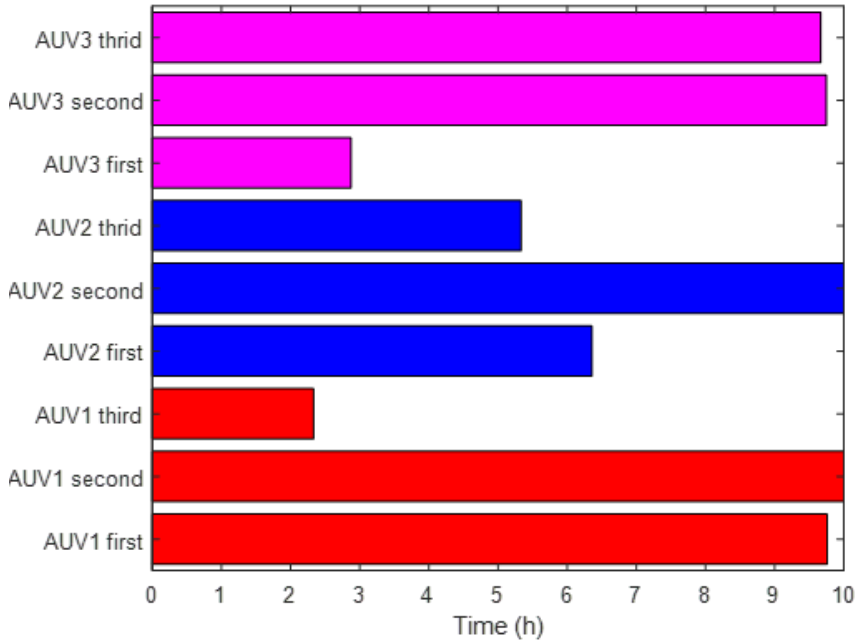

Figure 5.5: Operational time of each battery life for three AUVs.

The mission area is within the black square. Three AUVs and two ASVs are deployed from the asterisk point in Figure 5.4. We indicate the optimized trajectories of AUVs with colored dashed lines. The planned rendezvous locations of mobile chargers (ASVs) are shown as squares and circles. Numbers inside symbols represent the order of waypoints for each ASV. The mission completion time for three AUVs is 26.6 hours with the total travel distance of 199.5 km. In this mission, the two ASVs need to travel 39.1 km between all assigned rendezvous locations. Figure 5.5 shows all AUVs get recharged before running out of battery (maximum 10 hours).

We measure the mean values and standard deviations of mission completion time and travel distance of vehicles to show the reliability and efficiency of the pre-plan GA by analyzing the 100 results. The results show 31 out of 100 results have at least one ASV reaching the assigned rendezvous locations later than the AUV, which will cause a delay in the overall mission. The average mission completion time for those 31 results and the rest of 69 results are 28.6 hours and 28.3 hours respectively, with standard deviations of 1 hour and 1.1 hours. The average travel distance for those two cases are 204.4 km and 204.1 km with standard deviations of 1.6 km and 2.3 km. The late arrival of ASVs increases the total travel distance by 0.2% and delays the mission by 1%. This evaluation shows that even the GA cannot completely prevent the late arrival of ASVs, however, its impact on overall mission performance has been minimized. The results also show the proposed pre-plan GA is reliable: 34 results are within 5% of the best result, and 78 results are within 10% of the best result. The

GA performance on removing late arrival penalty and the reliability of GA can be balanced by changing weight ω.

To demonstrate the capability of integrating mission uncertainty into the proposed algorithm, the scenarios of AUV delay and failure for the pre-plan result in Figure 5.4 are simulated. We simulate the scenario where the operation of the second AUV (started with two thirds of battery, shown by blue lines) experiences a delay caused by environmental disturbances. Its arrival at the first rendezvous location is delayed from 0.1 to 2 hours and its effect is illustrated in Figure 5.6.

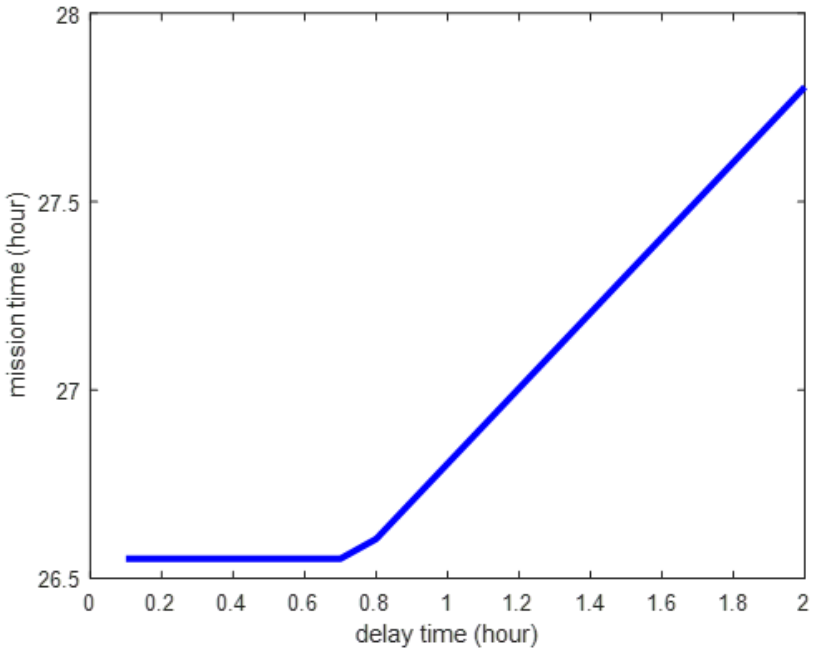

Figure 5.6: The relationship between the overall mission completion time and delay time of the first rendezvous of the second AUV.

Figure 5.6 shows the overall mission time rises from 26.6 hours to 27.8 hours with a 2 hour delay before the second AUV reaches its first rendezvous location. To remedy

the increase in mission completion time, the re-plan GA is implemented to optimize the trajectories of all three AUVs and two ASVs with the uncovered mission area. Because AUVs have limited communication underwater, the re-planned trajectories can only be applied at the rendezvous locations. Therefore, by the time a re-plan is performed, the trajectories of AUVs before meeting their next rendezvous locations are considered as covered mission area.

The uncovered mission area has 111 mission points. All AUVs will start with full battery from rendezvous locations with different starting times. Three AUVs will start at 11.8, 8.5, and 14.9 hours, which results in 37, 40, and 34 of mission points respectively. The re-plan GA will run 10 times with the rendezvous locations and times to find new trajectories. The best result is presented in Figure 5.7. The mission area covered by the three AUVs is indicated by colored solid lines. Waypoints traveled by two ASVs are represented by solid squares and circles. In this case, the result shows total mission time will be reduced to 27.6 hours if the rest of the mission is conducted following the re-plan GA result.

We further evaluate the re-plan GA performance by simulating a scenario where the second AUV has a complete failure at its first rendezvous location. The result of failure scenario re-planning is presented in Figure 5.8. In this case, the second AUV stops working and fails to follow the rest of its assigned trajectory. We implement the re-plan GA to this scenario with two AUVs and two ASVs to cover the rest of

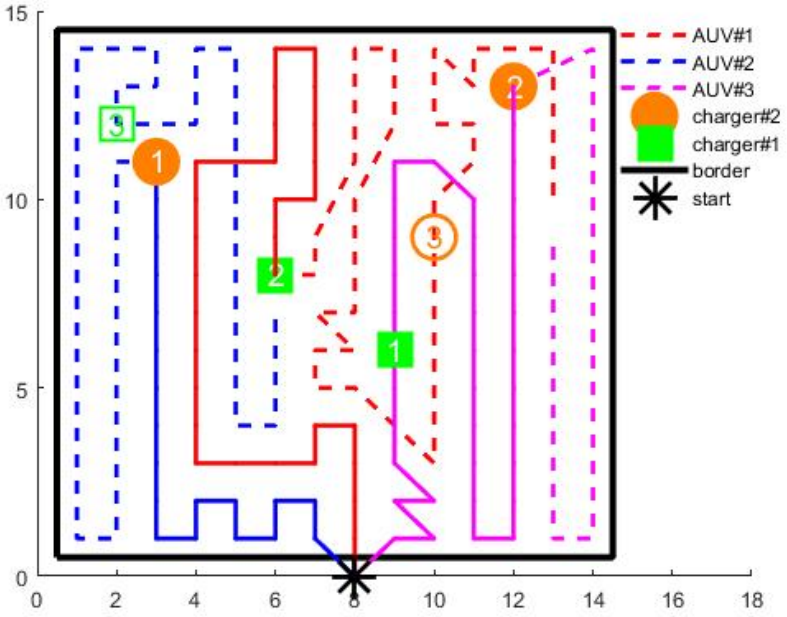

Figure 5.7: Re-plan optimizes trajectories of three AUVs and two ASVs to the rest of the mission area after 2 hours delay of an AUV.

the mission area. The result shows total mission time will be increased to 38.6 hours if the first and third AUVs continue to cover the rest of the mission area following the re-planned trajectories. Without the re-plan GA, the mission would fail.

The computational time for pre-plan GA is 2.3 minutes, and 0.3 minutes for the re-plan in the simulation scenario. The computational time of re-plan GA is related to the size of the remaining mission area. The computation speed of the re-plan GA is fast enough to be implemented multiple times during charging and transitions of vehicles. The improvement of re-plan results for compensating delay is insignificant in this simulation. It might be because only one delay is considered in simulation for the purpose of clear presentation. However, multiple delays and failures to AUVs can

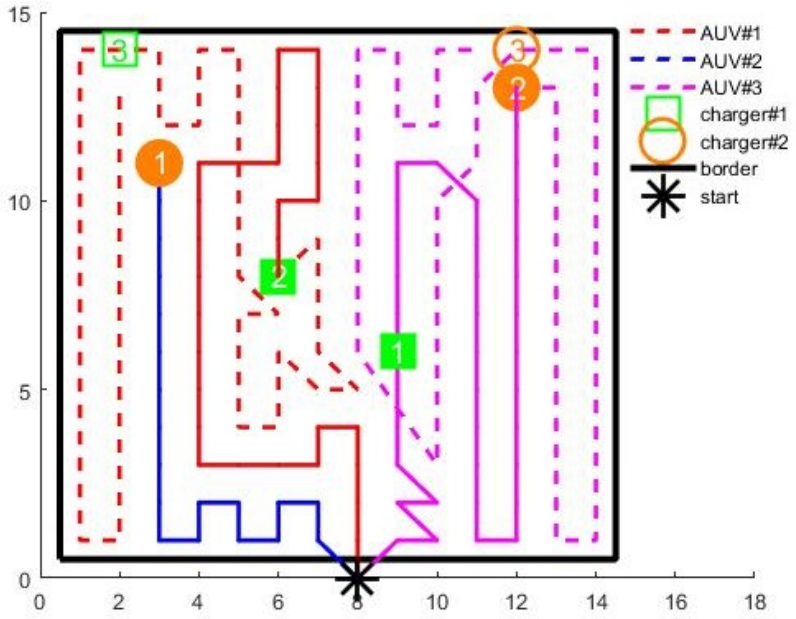

Figure 5.8: Re-plan optimizes trajectories of first, third AUVs and two ASVs to the rest of the mission area with the failure of the second AUV.

be handled with the same method, and the improvement will accumulate and become more obvious when more delays are considered.

According to the pre-plan evaluation, the proposed method successfully finds the trajectories of working robots and mobile chargers to minimize the mission completion time with high reliability. According to the re-plan evaluation, the proposed method could handle mission uncertainty by running the re-plan GA. The total mission time after applying the re-plan GA is shorter than continuing to use the pre-planned trajectories. In addition, a mission with a robot failure can still be completed without starting over again.

Chapter 6

Conclusion

This dissertation provides mission planning architectures for long-term missions using static and mobile charging stations. The approaches consider both overall mission performance and power consumption of the operating robots using information on area of operation, robot specifications, and environmental constraints.

For static energy replenishment, the mission planning problem is formulated to provide a solution that simultaneously generates trajectories for working robots, and places static charging stations to facilitate efficient energy cycling through the mission. The proposed method also accounts for obstacles, current, and can adapt to a priority search distribution. This developed method is applied to three mission scenarios. Simulation results demonstrate the effectiveness of the developed method

in both energy consumption and mission completion time. The capability of handling multiple mission constraints is also shown in the simulations. The robustness of the method is evaluated through Monte Carlo simulations. This work also enables the trade-off study to assist mission planners in evaluating impacts of parameters on the overall mission completion time and the total energy consumption.

In addition, a robotic network planning architecture for long-term missions utilizing mobile charging stations is proposed. The mobile charging stations can travel in the mission area to recharge the working robots before their batteries are depleted. The energy cost calculation of mobile charging stations is integrated with dynamic currents and obstacles into a multi-robot rendezvous planning approach, so that it can be applied to a variety of scenarios. With the authority of changing working robot trajectories, a GA based method is presented to optimize the trajectories of working robots and mobile charging stations. The developed method is tested in a variety of mission scenarios in dynamic environments. The results proved the reliability and efficiency of the method while validating the re-planing capability.

In the future, more constraints on robots and the environment will be considered. These constraints include energy limits on charging stations, collision avoidance between the robots, and characteristics of on-board sensors. Future work will include continuation of integration of the developed methods for real-world application and field experiments. The proposed method can be packaged as a software to generate

overall mission plan including waypoints of working agents, deployment of charging agents, and their charging scheduling. The software is implementable to different mission scenarios with a variety of constraints considering different mission configurations. The software can also be used as a guideline for evaluating the impacts of different mission objectives, and provide a trade-off analysis for different combinations of robots. These future implementations will provide us with better understanding of challenges and considerations needed for real-world missions such as air sampling missions and search and rescue missions.

References

[1] J. Kirk, "Multiple traveling salesmen problem - genetic algorithm, MATLAB Central File Exchange," 2014, https://www.mathworks.com/matlabcentral/fileexchange/19049-multiple-traveling-salesmen-problem-genetic-algorithm.

[2] R. Stokey, M. Purcell, N. Forrester, T. Austin, R. Goldsborough, B. Allen, and C. Von Alt, "A docking system for REMUS, an autonomous underwater vehicle," in *Proceedings MTS/IEEE Conference OCEANS*, 1997, pp. 1132–1136.

[3] J. M. Cena, "Power transfer efficiency of mutually coupled coils in an aluminum AUV hull," Master's thesis, Department of Electrical Engineering, Naval Postgraduate School, Monterey, CA, USA, 2013.

[4] A. Brighenti, L. Zugno, F. Mattiuzzo, and A. Sperandio, "EURODOCKER-a universal docking-downloading recharging system for AUVs: conceptual design results," in *Proceedings IEEE Conference OCEANS*, 1998, pp. 1463–1467.

[5] L. Angrisani, G. d'Alessandro, M. D'Arco, D. Accardo, and G. Fasano, "A contactless induction system for battery recharging of autonomous vehicles," in *Proceedings IEEE Conference MetroAeroSpace*, 2014, pp. 494–499.

[6] L. Angrisani, G. d'Alessandro, M. D'Arco, V. Paciello, and A. Pietrosanto, "Autonomous recharge of drones through an induction based power transfer system," in *Proceedings IEEE International Workshop on Measurements & Networking*, 2015, pp. 1–6.

[7] B. Fletcher, S. Martin, G. Flores, A. Jones, A. Nguyen, M. H. Brown, and D. L. Moore, "From the lab to the ocean: Characterizing the critical docking parameters for a free floating dock with a REMUS 600," in *Proceedings IEEE/MTS OCEANS–Anchorage*, 2017, pp. 1–7.

[8] D. Pyle, R. Granger, B. Geoghegan, R. Lindman, and J. Smith, "Leveraging a large UUV platform with a docking station to enable forward basing and persistence for light weight AUVs," in *Proceedings IEEE/MTS OCEANS*, 2012, pp. 1–8.

[9] Y. Mulgaonkar and V. Kumar, "Autonomous charging to enable long-endurance missions for small aerial robots," *Proceedings of SPIE-DSS*, p. 90831S, 2014.

[10] K. Leahy, D. Zhou, C.-I. Vasile, K. Oikonomopoulos, M. Schwager, and C. Belta, "Persistent surveillance for unmanned aerial vehicles subject to charging and

temporal logic constraints," *Autonomous Robots*, vol. 40, no. 8, pp. 1363–1378, 2016.

[11] N. Mathew, S. L. Smith, and S. L. Waslander, "Multirobot rendezvous planning for recharging in persistent tasks," *IEEE Transactions on Robotics*, vol. 31, no. 1, pp. 128–142, 2015.

[12] D. Mitchell, M. Corah, N. Chakraborty, K. Sycara, and N. Michael, "Multi-robot long-term persistent coverage with fuel constrained robots," in *Proceedings IEEE International Conference Robotics and Automation*, 2015, pp. 1093–1099.

[13] Z. Jin, T. Shima, and C. J. Schumacher, "Optimal scheduling for refueling multiple autonomous aerial vehicles," *IEEE Transactions on Robotics*, vol. 22, no. 4, pp. 682–693, 2006.

[14] R. Yehoshua, N. Agmon, and G. A. Kaminka, "Robotic adversarial coverage of known environments," *The International Journal of Robotics Research*, vol. 35, no. 12, pp. 1419–1444, 2016.

[15] M. Kapanoglu, M. Alikalfa, M. Ozkan, A. Yazıcı, and O. Parlaktuna, "A pattern-based genetic algorithm for multi-robot coverage path planning minimizing completion time," *Journal of Intelligent Manufacturing*, vol. 23, no. 4, pp. 1035–1045, 2012.

[16] B. R. Page, J. Naglak, C. Kase, and N. Mahmoudian, "Collapsible underwater

docking station: Design and evaluation," in *Proceedings MTS/IEEE OCEAN'S 18, Charleston, SC, October 21-25*, 2018.

[17] B. R. Page and N. Mahmoudian, "Simulation driven optimization of underwater docking station design," *IEEE Journal of Oceanic Engineering*, 2019.

[18] E. Galceran and M. Carreras, "A survey on coverage path planning for robotics," *Robotics and Autonomous Systems*, vol. 61, no. 12, pp. 1258–1276, 2013.

[19] H. Choset, "Coverage for robotics–a survey of recent results," *Annals of mathematics and artificial intelligence*, vol. 31, no. 1-4, pp. 113–126, 2001.

[20] A. Zelinsky, R. A. Jarvis, J. Byrne, and S. Yuta, "Planning paths of complete coverage of an unstructured environment by a mobile robot," in *Proceedings International Conference on Advanced Robotics*, vol. 13, 1993, pp. 533–538.

[21] Y. Gabriely and E. Rimon, "Spanning-tree based coverage of continuous areas by a mobile robot," *Annals of mathematics and artificial intelligence*, vol. 31, no. 1-4, pp. 77–98, 2001.

[22] C. Luo, S. X. Yang, D. A. Stacey, and J. C. Jofriet, "A solution to vicinity problem of obstacles in complete coverage path planning," in *Proceedings IEEE International Conference on Robotics and Automation*, vol. 1, 2002, pp. 612–617.

[23] S. L. Smith, M. Schwager, and D. Rus, "Persistent robotic tasks: Monitoring and

sweeping in changing environments," *IEEE Transactions on Robotics*, vol. 28, no. 2, pp. 410–426, 2012.

[24] J. M. Palacios-Gasós, E. Montijano, C. Sagüés, and S. Llorente, "Distributed coverage estimation and control for multirobot persistent tasks," *IEEE Transactions on Robotics*, vol. 32, no. 6, pp. 1444–1460, 2016.

[25] J. Keller, D. Thakur, M. Likhachev, J. Gallier, and V. Kumar, "Coordinated path planning for fixed-wing UAS conducting persistent surveillance missions," *IEEE Transactions on Automation Science and Engineering*, vol. 14, no. 1, pp. 17–24, 2017.

[26] F. Pasqualetti, J. W. Durham, and F. Bullo, "Cooperative patrolling via weighted tours: Performance analysis and distributed algorithms," *IEEE Transactions on Robotics*, vol. 28, no. 5, pp. 1181–1188, 2012.

[27] D. E. Soltero, M. Schwager, and D. Rus, "Decentralized path planning for coverage tasks using gradient descent adaptive control," *The International Journal of Robotics Research*, vol. 33, no. 3, pp. 401–425, 2014.

[28] C. Song, L. Liu, G. Feng, Y. Wang, and Q. Gao, "Persistent awareness coverage control for mobile sensor networks," *Automatica*, vol. 49, no. 6, pp. 1867–1873, 2013.

[29] N. Mathew, S. L. Smith, and S. L. Waslander, "A graph-based approach to

multi-robot rendezvous for recharging in persistent tasks," in *Proceedings IEEE International Conference Robotics and Automation*, 2013, pp. 3497–3502.

[30] P. Zebrowski and R. T. Vaughan, "Recharging robot teams: A tanker approach," in *Proceedings IEEE International Conference Advanced Robotics*, 2005, pp. 803–810.

[31] Y. Litus, R. T. Vaughan, and P. Zebrowski, "The frugal feeding problem: Energy-efficient, multi-robot, multi-place rendezvous," in *Proceedings IEEE International Conference Robotics and Automation*, 2007, pp. 27–32.

[32] Y. Litus, P. Zebrowski, and R. T. Vaughan, "A distributed heuristic for energy-efficient multirobot multiplace rendezvous," *IEEE Transactions on Robotics*, vol. 25, no. 1, pp. 130–135, 2009.

[33] P. Maini and P. Sujit, "On cooperation between a fuel constrained UAV and a refueling UGV for large scale mapping applications," in *Proceedings IEEE International Conference on Unmanned Aircraft Systems*, 2015, pp. 1370–1377.

[34] W. Ho, G. T. Ho, P. Ji, and H. C. Lau, "A hybrid genetic algorithm for the multi-depot vehicle routing problem," *Engineering Applications of Artificial Intelligence*, vol. 21, no. 4, pp. 548–557, 2008.

[35] P. Surekha and S. Sumathi, "Solution to multi-depot vehicle routing problem using genetic algorithms," *World Applied Programming*, vol. 1, no. 3, pp. 118–131, 2011.

[36] M. A. Batalin and G. S. Sukhatme, "The design and analysis of an efficient local algorithm for coverage and exploration based on sensor network deployment," *IEEE Transactions on Robotics*, vol. 23, no. 4, pp. 661–675, 2007.

[37] D. Rao and S. B. Williams, "Large-scale path planning for underwater gliders in ocean currents," in *Australasian Conference on Robotics and Automation (ACRA)*, 2009.

[38] D. Kularatne, S. Bhattacharya, and M. A. Hsieh, "Time and energy optimal path planning in general flows." in *Robotics: Science and Systems*, 2016.

[39] Y. Hu and S. X. Yang, "A knowledge based genetic algorithm for path planning of a mobile robot," in *Proceedings IEEE International Conference Robotics and Automation*, vol. 5, 2004, pp. 4350–4355.

[40] B. Li, B. Moridian, and N. Mahmoudian, "Underwater multi-robot persistent area coverage mission planning," in *Proceedings MTS/IEEE Conference OCEANS*, 2016, pp. 1–6.

[41] A. Konak, D. W. Coit, and A. E. Smith, "Multi-objective optimization using genetic algorithms: A tutorial," *Reliability Engineering & System Safety*, vol. 91, no. 9, pp. 992–1007, 2006.

[42] J. A. Hartigan and M. A. Wong, "Algorithm as 136: A k-means clustering algorithm," *Journal of the Royal Statistical Society. Series C (Applied Statistics)*, vol. 28, no. 1, pp. 100–108, 1979.

[43] B. Li, B. Moridian, A. Kamal, S. Patankar, and N. Mahmoudian, "Multi-robot mission planning with static energy replenishment," *Journal of Intelligent & Robotic Systems doi.org/10.1007/s10846-018-0897-2*, pp. 1–15, 2018.

[44] B. Li, S. Patankar, B. Moridian, and N. Mahmoudian, "Planning large-scale search and rescue using team of UAVs and charging stations," in *Proceedings IEEE International Symposium on Safety, Security, and Rescue Robotics*, 2018, pp. 1–8.

[45] B. Li, B. Moridian, and N. Mahmoudian, "Autonomous oil spills detection: Mission planning for ASVs and AUVs with static recharging," in *Proceedings MTS/IEEE OCEAN'S 18, Charleston, SC, October 21-25*, 2018.

[46] A. Inzartsev, A. Pavin, and N. Rylov, "Development of the AUV automatic docking methods based on echosounder and video data," in *IEEE 24th Saint Petersburg International Conference on Integrated Navigation Systems (ICINS)*, 2017, pp. 1–6.

[47] M. Wirtz, M. Hildebrandt, and C. Gaudig, "Design and test of a robust docking system for hovering AUVs," in *Proceedings IEEE/MTS OCEANS*, 2012, pp. 1–6.

[48] T. Kawasaki, T. Fukasawa, T. Noguchi, and M. Baino, "Development of AUV "Marine Bird" with underwater docking and recharging system," in *IEE 3rd International Workshop on Scientific Use of Submarine Cables and Related Technologies*, 2003, pp. 166–170.

[49] K. Yu, A. K. Budhiraja, and P. Tokekar, "Algorithms for routing of unmanned aerial vehicles with mobile recharging stations and for package delivery," *arXiv preprint arXiv:1704.00079*, 2017.

[50] D. N. Subramani and P. F. Lermusiaux, "Energy-optimal path planning by stochastic dynamically orthogonal level-set optimization," *Ocean Modelling*, vol. 100, pp. 57–77, 2016.

[51] Y.-S. Jung, K.-W. Lee, S.-Y. Lee, M. H. Choi, and B.-H. Lee, "An efficient underwater coverage method for multi-AUV with sea current disturbances," *International Journal of Control, Automation and Systems*, vol. 7, no. 4, pp. 615–629, 2009.

[52] V. T. Huynh, M. Dunbabin, and R. N. Smith, "Predictive motion planning for auvs subject to strong time-varying currents and forecasting uncertainties," in *IEEE International Conference on Robotics and Automation (ICRA)*, 2015, pp. 1144–1151.

[53] O. A. Yakimenko, D. P. Horner, and D. G. Pratt, "AUV rendezvous trajectories generation for underwater recovery," in *Proceedings IEEE 16th Mediterranean Conference on Control and Automation*, 2008, pp. 1192–1197.

[54] S. MahmoudZadeh, A. Yazdani, K. Sammut, and D. Powers, "Online path planning for AUV rendezvous in dynamic cluttered undersea environment using evolutionary algorithms," *Applied Soft Computing*, 2017.

[55] S. Lin and B. W. Kernighan, "An effective heuristic algorithm for the traveling-salesman problem," *Operations research*, vol. 21, no. 2, pp. 498–516, 1973.

[56] Y. Gabriely and E. Rimon, "Spiral-stc: An on-line coverage algorithm of grid environments by a mobile robot," in *Proceedings IEEE International Conference on Robotics and Automation*, vol. 1, 2002, pp. 954–960.

[57] Y. Bouzid, Y. Bestaoui, and H. Siguerdidjane, "Quadrotor-UAV optimal coverage path planning in cluttered environment with a limited onboard energy," in *Proceedings IEEE/RSJ International Conference on Intelligent Robots and Systems*, 2017.

[58] C. Di Franco and G. Buttazzo, "Energy-aware coverage path planning of UAVs," in *Proceedings IEEE International Conference on Autonomous Robot Systems and Competitions*, 2015, pp. 111–117.

[59] Y. Mei, Y.-H. Lu, Y. C. Hu, and C. G. Lee, "Deployment of mobile robots with energy and timing constraints," *IEEE Transactions on robotics*, vol. 22, no. 3, pp. 507–522, 2006.

[60] N. Kamra, T. S. Kumar, and N. Ayanian, "Combinatorial problems in multi-robot battery exchange systems," *IEEE Transactions on Automation Science and Engineering*, 2017.

[61] F. Arvin, K. Samsudin, and A. R. Ramli, "Swarm robots long term autonomy using moveable charger," in *Proceedings IEEE International Conference on Future Computer and Communication*, 2009, pp. 127–130.

[62] J. Van Den Berg, D. Ferguson, and J. Kuffner, "Anytime path planning and replanning in dynamic environments," in *Proceedings IEEE International Conference on Robotics and Automation (ICRA)*, 2006, pp. 2366–2371.

Appendix A

Letter of Permission

SPRINGER NATURE LICENSE
TERMS AND CONDITIONS

Nov 29, 2018

This Agreement between Bingxi Li ("You") and Springer Nature ("Springer Nature") consists of your license details and the terms and conditions provided by Springer Nature and Copyright Clearance Center.

License Number	4478380804515
License date	Nov 29, 2018
Licensed Content Publisher	Springer Nature
Licensed Content Publication	Journal of Intelligent and Robotic Systems
Licensed Content Title	Multi-Robot Mission Planning with Static Energy Replenishment
Licensed Content Author	Bingxi Li, Barzin Moridian, Anurag Kamal et al
Licensed Content Date	Jan 1, 2018
Type of Use	Thesis/Dissertation
Requestor type	academic/university or research institute
Format	print and electronic
Portion	full article/chapter
Will you be translating?	no
Circulation/distribution	<501
Author of this Springer Nature content	yes
Title	MULTI-ROBOT MISSION PLANNING WITH ENERGY REPLENISHMENT
Institution name	Michigan Technological University
Expected presentation date	Jan 2020
Requestor Location	Bingxi Li 1804 Woodmar Dr. F HOUGHTON, MI 49931 United States Attn: Bingxi Li
Billing Type	Invoice
Billing Address	Bingxi Li 1804 Woodmar Dr. F HOUGHTON, MI 49931 United States Attn: Bingxi Li
Total	0.00 USD
Terms and Conditions	

Springer Nature Terms and Conditions for RightsLink Permissions

Springer Nature Customer Service Centre GmbH (the Licensor) hereby grants you a non-exclusive, world-wide licence to reproduce the material and for the purpose and

requirements specified in the attached copy of your order form, and for no other use, subject to the conditions below:

1. The Licensor warrants that it has, to the best of its knowledge, the rights to license reuse of this material. However, you should ensure that the material you are requesting is original to the Licensor and does not carry the copyright of another entity (as credited in the published version).

   If the credit line on any part of the material you have requested indicates that it was reprinted or adapted with permission from another source, then you should also seek permission from that source to reuse the material.

2. Where **print only** permission has been granted for a fee, separate permission must be obtained for any additional electronic re-use.

3. Permission granted **free of charge** for material in print is also usually granted for any electronic version of that work, provided that the material is incidental to your work as a whole and that the electronic version is essentially equivalent to, or substitutes for, the print version.

4. A licence for 'post on a website' is valid for 12 months from the licence date. This licence does not cover use of full text articles on websites.

5. Where **'reuse in a dissertation/thesis'** has been selected the following terms apply: Print rights of the final author's accepted manuscript (for clarity, NOT the published version) for up to 100 copies, electronic rights for use only on a personal website or institutional repository as defined by the Sherpa guideline (www.sherpa.ac.uk/romeo/).

6. Permission granted for books and journals is granted for the lifetime of the first edition and does not apply to second and subsequent editions (except where the first edition permission was granted free of charge or for signatories to the STM Permissions Guidelines http://www.stm-assoc.org/copyright-legal-affairs/permissions/permissions-guidelines/), and does not apply for editions in other languages unless additional translation rights have been granted separately in the licence.

7. Rights for additional components such as custom editions and derivatives require additional permission and may be subject to an additional fee. Please apply to Journalpermissions@springernature.com/bookpermissions@springernature.com for these rights.

8. The Licensor's permission must be acknowledged next to the licensed material in print. In electronic form, this acknowledgement must be visible at the same time as the figures/tables/illustrations or abstract, and must be hyperlinked to the journal/book's homepage. Our required acknowledgement format is in the Appendix below.

9. Use of the material for incidental promotional use, minor editing privileges (this does not include cropping, adapting, omitting material or any other changes that affect the meaning, intention or moral rights of the author) and copies for the disabled are permitted under this licence.

10. Minor adaptations of single figures (changes of format, colour and style) do not require the Licensor's approval. However, the adaptation should be credited as shown in Appendix below.

Appendix — Acknowledgements:

For Journal Content:
Reprinted by permission from [**the Licensor**]: [**Journal Publisher** (e.g. Nature/Springer/Palgrave)] [**JOURNAL NAME**] [**REFERENCE CITATION** (Article name, Author(s) Name), [**COPYRIGHT**] (year of publication)